AD-A149 016 ELECTROMAGNETIC INSPECTION OF WIRE ROPES USING SENSOR ARRAYS(U) NDT TECHNOLOGIES INC SOUTH WINDSOR CT H R WEISCHEDEL 05 NOV 84 N00014-83-C-0484 1/1

UNCLASSIFIED F/G 11/6 NL

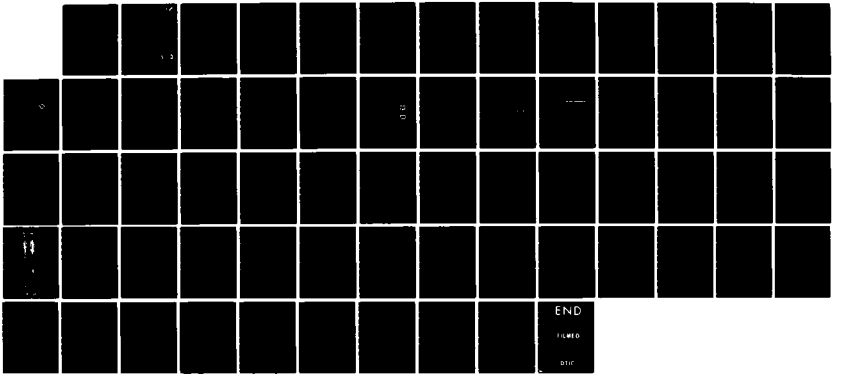

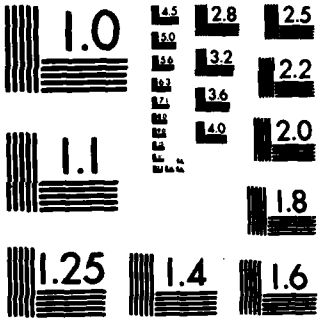

Contract N00014-83-C-0484

ELECTROMAGNETIC INSPECTION OF WIRE ROPES USING SENSOR ARRAYS

Herbert R. Weischedel
NDT Technologies, Inc.
P.O.Box 637
150 Strong Road
South Windsor, CT 06074

5 November 1984

Annual Summary Report for Period
16 June 1983 - 15 June 1984

Prepared for

OFFICE OF NAVAL RESEARCH
DEPARTMENT OF THE NAVY
800 N. Quincy Street
Arlington, Virginia 22217

A.W. TII 1/24/85

AD AD A149018 (U) FIELD/GROUP P11/6 - cr. P13/8 - cr. S20/3 - cr.

UNCLASSIFIED TITLE

ELECTROMAGNETIC INSPECTION OF WIRE ROPES USING SENSOR ARRAYS.

ABSTRACT

(U) WE DEVELOPED A NEW QUANTITATIVE PROCEDURE AND INSTRUMENTATION FOR THE INSPECTION OF WIRE ROPES. TO GAIN A BETTER U NDERSTANDING OF THE INSTRUMENT PERFORMANCE, WE UNDERTOOK AN EXPERIMENTAL INVESTIGATION OF THE MAGNETIC FLUX PATTERNS IN SIDE THE INSTRUMENT AND WIRE ROPE. USING AN IBM PERSONNEL COMPUTER IN COMBINATION WITH APPROPRIATE INTERFACE HARDWARE, WE IMPLEMENTED COMPUTER-AIDED DEFECT IDENTIFICATION METHODS. THESE METHODS ARE PRESENTLY BEING IMPROVED AND EXTENDED. W E PERFORMED FIRST EXPERIMENTS TO IMPLEMENT METHODS FOR THE INSPECTION OF WIRE ROPE END SECTIONS, CLOSE TO THE ROPE TERM INATIONS. THESE EXPERIMENTS INDICATE THAT AN INSTRUMENT OF THIS TYPE IS FEASIBLE. A PROTOTYPE IS PRESENTLY BEING IMPLEM ENTED. WE DELIVERED TWELVE SMLL INSTRUMENTS OF THE NEW DESIGN TO THE US NAVY. THEY ARE PRESENTLY BEING SUCCESSFULLY USE D BY VARIOUS NAVY PERSONNEL. ADDITIONAL INSTRUMENTS OF THE NEW DESIGN WERE SOLD TO THE MINE SAFETY AND HEALTH ADMINISTR ATION, THE SCRIPPS INSTITUTE OF OCEANOGRAPHY, THE UNIVERSITY OF RHODE ISLAND, THE BRITISH NATIONAL COAL BOARD, AND THE KONE ELEVATOR COMPANY.

POSTING TERMS ASSIGNED

BRITISH NATIONAL COAL BOARD
  USE COAL
      GREAT BRITAIN

ELECTROMAGNETIC INSPECTION
  USE ELECTROMAGNETISM - cr.
  * INSPECTION - cr.

HEALTH ADMINISTRATION
  USE HEALTH

INTERFACE HARDWARE
  USE INTERFACES

MINE SAFETY
  USE MINES(EXCAVATIONS)
      SAFETY

NEW QUANTITATIVE PROCEDURE
  USE QUANTITATIVE ANALYSIS

COMPUTER-AIDED DEFECT IDENTIFICATION METHODS
  USE * COMPUTER AIDED DIAGNOSIS - cr.
      DEFECTS(MATERIALS) - cr.
      IDENTIFICATION SYSTEMS
      * Test equipment - cr.

ELEVATOR COMPANY
  USE COMPANY LEVEL ORGANIZATIONS
      ELEVATORS

INSPECTION OF WIRE ROPES
  USE INSPECTION
      ROPE
      WIRE
      * Wire rope - cr.

MAGNETIC FLUX PATTERNS
  USE FLUX(RATE) - cr.
      MAGNETIC FIELDS - cr.
      PATTERNS

NAVY PERSONNEL
  USE NAVAL PERSONNEL

OCEANOGRAPHY
  USE OCEANOGRAPHY

PERSONNEL COMPUTER
USE COMPUTERS
PERSONNEL

SENSOR ARRAYS
USE ARRAYS
DETECTORS

WIRE ROPE
USE ROPE
WIRE

WIRE ROPES
USE ROPE
WIRE

ROPE TERMINATIONS
USE ROPE

UNIVERSITY OF RHODE ISLAND
USE RHODE ISLAND
UNIVERSITIES

WIRE ROPE END SECTIONS
USE ROPE
WIRE

PHRASES NOT FOUND DURING LEXICAL DICTIONARY MATCH PROCESS

1. SUMMARY

During the first year of the present contract, we developed a new quantitative procedure and instrumentation for the inspection of wire ropes. The new instruments have the following properties:

- The quantitative determination of loss of metallic cross-sectional area (LMA) caused by localized flaws (e.g., broken wires) and by distributed flaws (e.g., corrosion or abrasion) is possible with a quantitative resolution of 50 mm. (Here, "quantitative resolution" is defined as the required minimum flaw length for which the sensor provides a quantitative measure of LMA directly, without additional signal processing).

- The qualitative detection of flaws shorter than 50 mm is possible without further signal processing.

- Using a computer aided quantitative defect identification method, the quantitative resolution can be further improved to approximately 10 mm. For shorter flaws, a slightly less accurate estimate of LMA is still available.

- As compared to previous state-of-the-art instruments, the quantitative resolution of the new instruments was improved from approximately 750 mm to 50 mm, a factor of 15.

- As compared to the previous air coils, the use of sense coils with ferrous cores gives an improved signal-to-noise ratio and signal repeatability.

To gain a better understanding of the instrument performance, we undertook an experimental investigation of the magnetic flux patterns inside the instrument and wire rope.

Using an IBM Personal Computer in combination with appropriate interface hardware, we implemented computer-aided defect identification methods. These methods are presently being improved and extended.

We performed first experiments to implement methods for the inspection of wire rope end sections, close to the rope terminations. These experiments indicate that an instrument of this type is feasible. A prototype is presently being implemented.

We delivered twelve small instruments of the new design to the US Navy. They are presently being successfully used by various Navy personnel. Additional instruments of the new design were sold to the Mine Safety and Health Administration, the Scripps Institute of Oceanography, the University of Rhode Island, the British National Coal Board, and the Kone Elevator Company.

2. INTRODUCTION

The principal and most prevalent deterioration modes of wire rope can be summarized as follows:

(i) Abrasion (external)
caused by rubbing along floor or other surfaces.

Abrasion (internal)
caused by nicking, high pressures, poor lubrication

(ii) Corrosion (external,internal)
caused by environmental conditions, poor lubrication

(iii) Broken Wires
caused by fatigue, plastic wear, martensitic embrittlement, mechanical damage

(iv) Kinks and other Mechanical Damage

Electromagnetic inspection methods can detect these flaws. While it should not completely replace careful visual inspections, nondestructive testing provides great insight on the condition of a rope. During the past 40 years, it has gradually become an accepted method for the inspection of wire ropes in the mining industry and for ski lifts in North America, Europe, and South Africa.

Two different types of nondestructive inspection methods have evolved: Localized Fault (LF) inspection and inspection for Loss of Metallic Cross-Sectional Area (LMA).

LF inspection is more suitable for the qualitative detection of localized flaws such as broken wires. The LMA inspection method is better suited for the detection and quantitative evaluation of distributed flaws such as abrasion and corrosion.

The first LF instruments for the inspection of wire ropes were developed approximately in 1935. These instruments were also called "DC" or "leakage flux" instruments. The basic principles are still being used in most of the present nondestructive wire rope inspection instruments, especially in Europe [1]-[19]. The technique used in leakage flux testing, shown in Figure 1, is to magnetically saturate a section of the steel rope in the longitudinal direction by strong permanent or electric magnets. Wherever there is an discontinuity in the rope such as a broken wire, a broken core, corrosion or abrasion, the magnetic flux is distorted and leaks from the rope. Sense coils or Hall generators, close to the rope, sense the leakage flux. The rope moves which causes the changing flux to intersect the sensors. The changing flux induces voltages in the coils or Hall generators. The sensor voltages are suitably combined and processed to produce the test signals. LF type instruments allow only a qualitative detection of localized faults such as broken wires or corrosion pitting. A quantitative estimate of rope deterioration is not available. Detection of internal and external abrasion is usually not possible.

The first LMA type instruments were developed as early as 1907. These instruments were also called "AC" instruments because they use AC magnetization of the rope as in Figure 2. They are very similar to the well-known eddy current NDT instruments. A wide variety of implementations of the basic principles are known [17], [20], [21], [22]. In these instruments, the wire rope serves substantially as the ferrous core of a coil or a transformer. A changing rope cross section changes the impedance

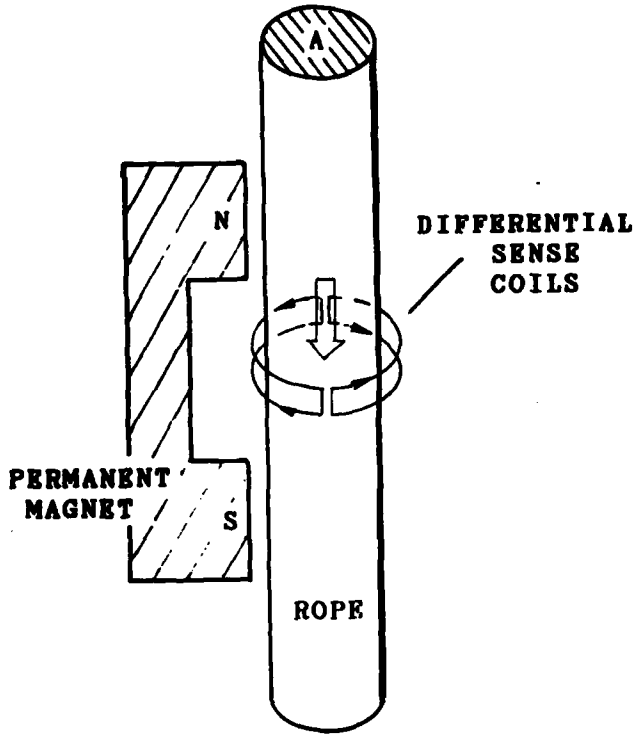

Figure 1: Leakage Flux Method
with Differential Coils

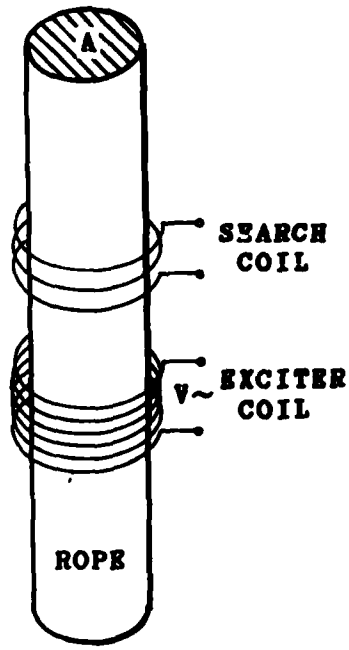

Figure 2: AC Main Flux Method

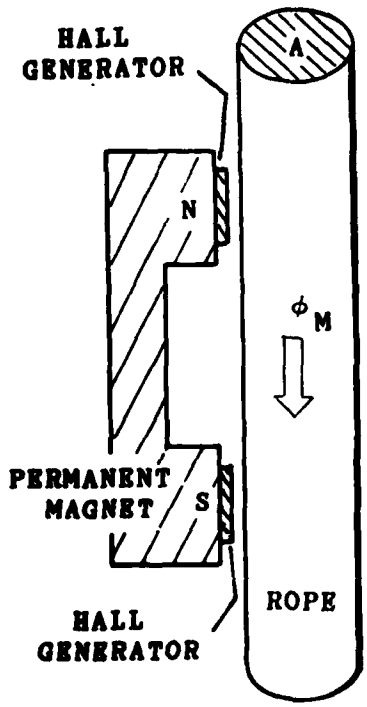

Figure 3: DC Main Flux Method
with Hall Generators
in Air Gap

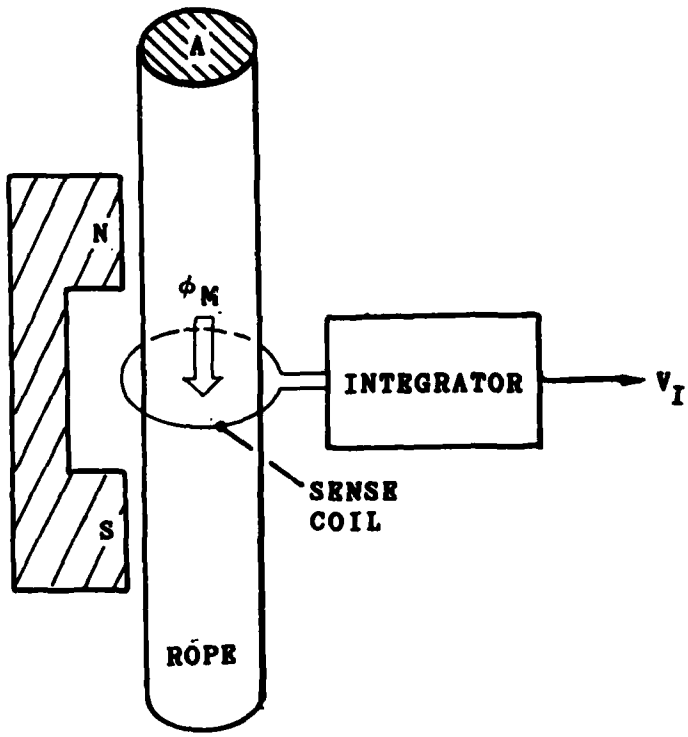

Figure 4: DC Main Flux Method
with Sense Coil on Rope

of the test arrangement. The changing impedance serves as a measure of the rope cross-sectional area. In spite of many improvements, AC testing suffers from serious deficiencies such as insufficient resolution and unreliability. However, it gives at least an estimate of actual rope deterioration.

An LMA instrument using Hall generators was developed in 1979 [22], [23], [24]. This instrument uses dc magnetization of the rope and measures the magnetic main flux in the rope. Therefore it could be called a "dc main flux " instrument. Figure 3 illustrates the principles used. Similar to the LF method, strong permanent magnets induce a longitudinal magnetic flux in the rope. Hall generators are positioned in the air gap between the permanent magnet and the rope. They sense the flux density in the air gap which is a function of the rope volume between the poles. The flux density in the air gap is therefore a measure of the average metallic cross-sectional area of the rope section between the poles. In addition to the LMA sensor, an LF sensor is also incorporated in this instrument. An instrument using somewhat similar principles together with sense coils was developed in Switzerland in 1972 [17].

Although this combined LMA/LF instrument represents a considerable improvement over the above mentioned AC test instruments, it still suffers from rather low qualitative resolving power. The qualitative resolving power depends on the distance of the magnetic poles, and the instrument measures only an average value of the rope's metallic cross section between the poles. It cannot detect and quantitatively evaluate geometrically small or even medium sized flaws such as localized corrosion, abrasion, or clusters of broken wires. Since most corrosion and

abrasion occurs in localized patches, an actual estimate of remaining rope strength based on these LMA measurements is unreliable. Remarkably, quantitative estimates of remaining rope strength, based on these instruments, rely to a considerable extent on the (qualitative) LF signal rather than the (quantitative) LMA signal (see Reference [25]).

A new class of dc main-flux instruments for the quantitative determination of loss of metallic cross-sectional area was developed under the present contract [1]. These new LMA/LF instruments overcome most problems of previous LMA instruments. Their quantitative resolving power is better by an order of magnitude than that of any of the previous instruments. The new wire rope test instruments for the quantitative determination of loss of metallic cross-sectional area are described in the following.

3. MAIN FLUX INSTRUMENT FOR THE QUANTITATIVE DETERMINATION OF WIRE ROPE CROSS-SECTIONAL AREA

3.1 Operating Principles

Figure 4 illustrates the underlying principles of the new LMA/LF method [1]. Similar to the previous LF instruments, permanent magnets induce a magnetic dc flux in the wire rope in the longitudinal direction, and they magnetically saturate the rope. A concentric coil surrounds the rope. The rope then moves. Any change of the metallic cross-sectional area A of the rope (caused by flaws such as corrosion, abrasion or broken wires) causes a change of the main flux Φ_M in the rope. Hence, as the rope moves, the changing main flux induces a voltage in the test coil which is

proportional to the derivative of the magnetic flux ϕ_M. The induced voltage is integrated by the integrator circuit. The output voltage of the integrator circuit v_I is then a voltage directly proportional to the main flux ϕ_M. Since the rope is magnetically saturated, the main flux is directly proportional to the instantaneous cross-sectional area of the rope. Hence a change of v_I is a measure of the change in metallic cross-sectional area A.

The approach shown in Figure 4 was recently also proposed, independently, in [22]. However, the arrangement of Figure 4 is hardly feasible and clearly not practical because the search coil cannot be subdivided and hinged. A subdivision of the search coil is absolutely necessary to facilitate mounting the instrument on the rope. To solve this problem, we used a novel approach which is explained by using Figure 5.

Note that the configurations shown in Figure 4 and Figure 5a are identical. The arrangement in Figure 5a is now augmented by an additional coil (i.e., Coil 2) in Figure 5b. The net flux linkages in Coil 2 are substantially zero at all times, and only negligible voltages are induced in this coil as the rope moves. Hence, adding the Coil 2 voltage (which is approximately zero) to the Coil 1 voltage obviously leaves the Coil 1 voltage substantially unchanged. Coils 1 and 2 are now rearranged as shown in Figure 5c. Following the above argumentation, it is easy to see that the combined voltages induced in the Upper and Lower Coils in Figure 5c are substantially equal to the voltage induced in Coil 1 of Figure 5a. An instrument with this new coil configuration can be hinged which makes it easy to mount it on the rope. Furthermore, we can now wind the upper and

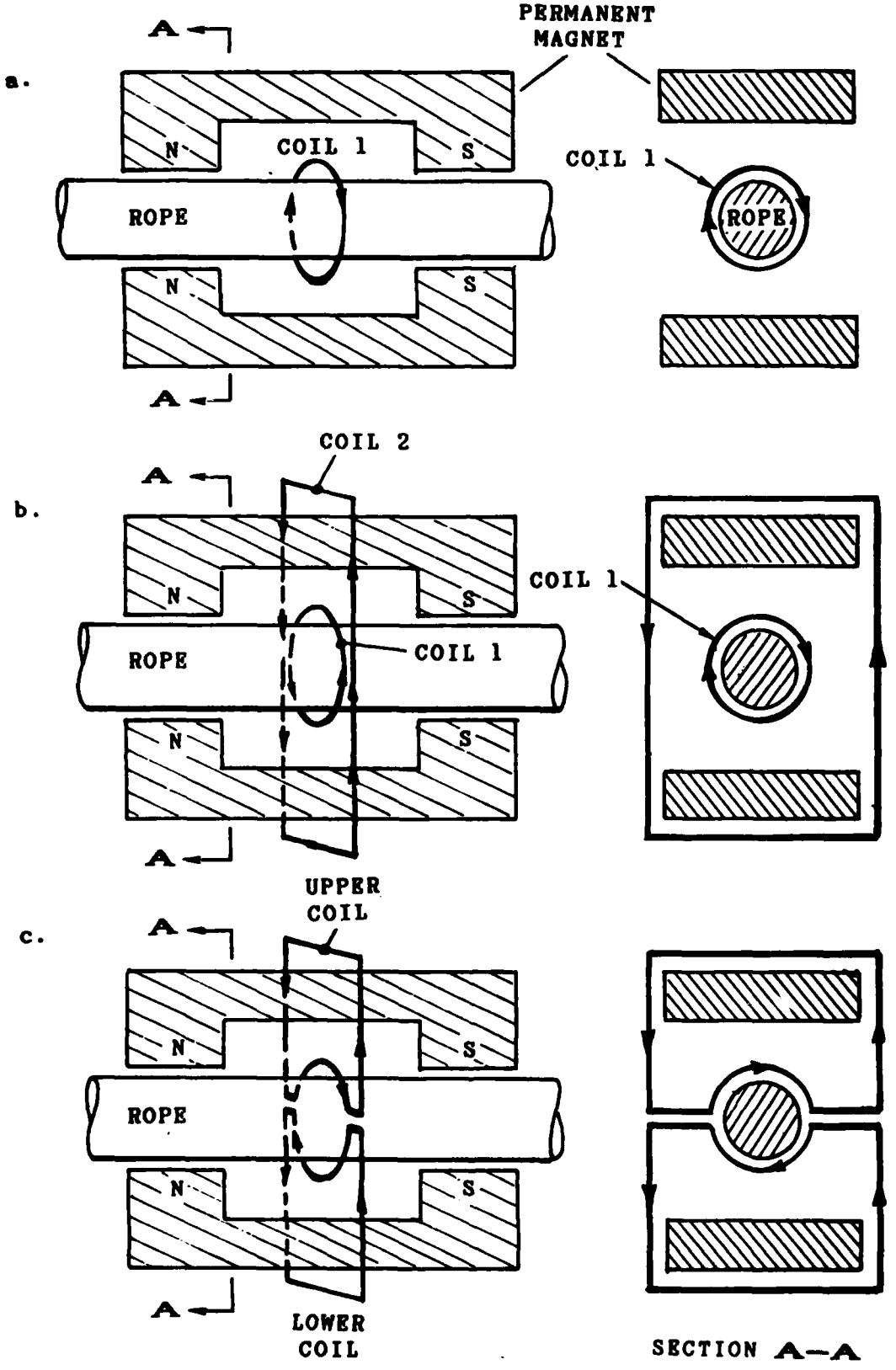

Figure 5: New DC Main Flux Instrument with Hinged Sense Coil

lower coils with a large number of turns (several thousand). Hence coil voltages can be in the millivolt range, which greatly facilitates the difficult problem of a long-term low-drift integration required by the implemented approach.

The problem of intrinsic noise, caused by the inhomogeneous rope structure combined with the subdivided and hinged air coil arrangement, was discussed in [1], [2]. The intrinsic noise can cause a low signal-to-noise ratio in many cases. In [1], we proposed a solution of this problem by using sense coils with ferrous cores. A ferrous core can eliminate the magnetic discontinuities caused by the subdivided and hinged air coils. Therefore, the sense coils of the implemented LMA instruments are wound on ferrous cores to eliminate the intrinsic noise caused by the inhomogeneous rope structure. Figure 6 shows this arrangement. As we have previously discussed in [1], the ferrous core guides all the magnetic leakage flux through the coils, and it eliminates the effects of discontinuities of the sense coil introduced by its subdivision.

Based on the above observations and on tests using the new LMA/LF instruments, we can summarize the main features of the implemented Main Flux Method:

- The reduction of metallic cross-sectional area caused by continuous defects, such as abrasion and corrosion, can be determined quantitatively with excellent resolution.

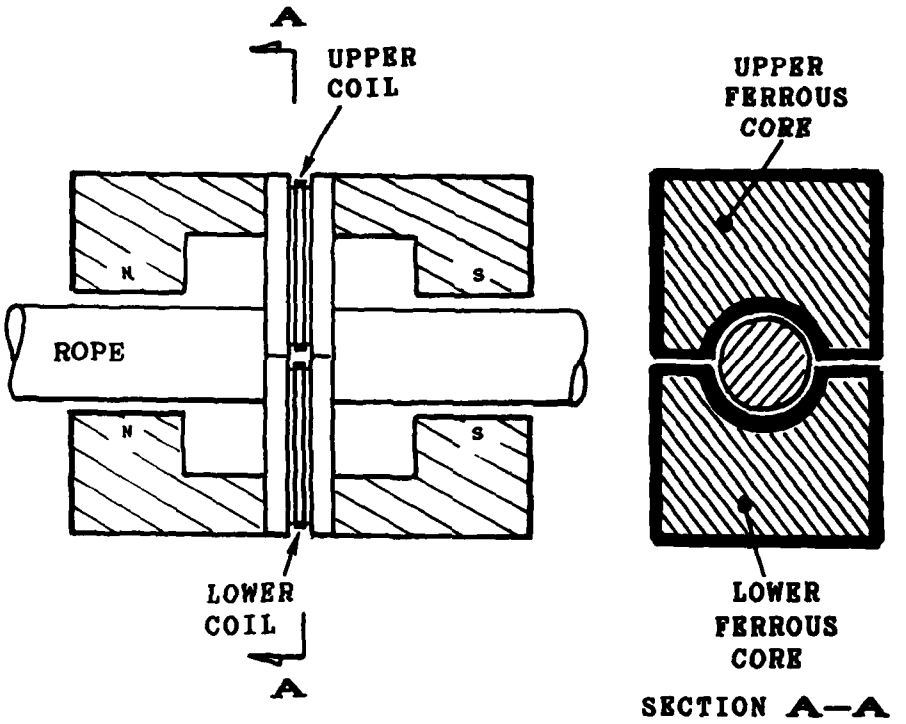

Figure 6: Coils with Ferrous Cores

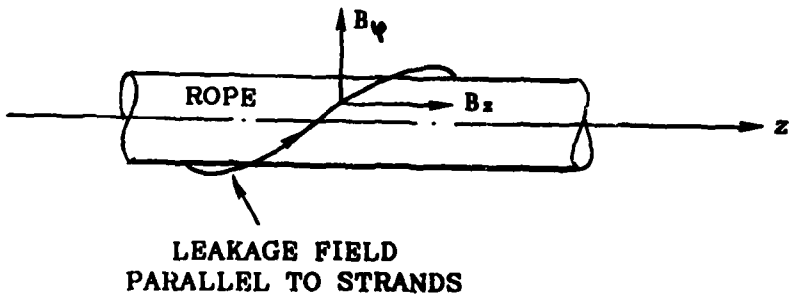

Figure 7: Azimuthal Leakage Field

- The reduction of metallic cross-sectional area caused by broken wires with gap lengths longer than approximately 2 inches can be determined quantitatively.

- Localized defects, such as broken wires with gap lengths less than approximately 2 inches, can be qualitatively detected.

- Using a computer assisted quantitative defect identification method, a quantitative evaluation of localized flaws with any gap length is possible.

- Because of the high Penetration Ratio of the sensor (a definition of "Penetration Ratio" is given in the next chapter), the signal-to-noise ratio and penetration depth is better than that of most presently available leakage flux instruments using differential coils.

- The Quantitative Resolution (as defined in the next chapter) of the new instruments is better by an order of magnitude than that of any previous instrument.

- Signal amplitudes are independent of rope speed.

The design and performance of the new LMA instruments is discussed in the following chapter.

3.2 Sense Coil Design

For a rational sensor design and to allow a comparison of the performance of different sensors, we have formulated the following performance criteria:

1. Resolution. The Resolution of a transducer is measured by the the smallest distance between flaws for which the transducer provides distinctly separate flaw indications. Resolving Power is defined as the reciprocal of the resolution.

2. Quantitative Resolution. The Quantitative Resolution is the required minimum length of a uniform flaw for which the sensor provides a quantitative measurement of the absolute change of metallic cross-sectional area within a predefined small error limit (for the present report, we used an error limit of approximately 5%). Quantitative Resolving Power is defined as the reciprocal of the Quantitative Resolution. Because all sensors have finite quantitative resolving power, minimum flaw dimensions are always required for an accurate quantitative fault identification. The concept of "quantitative resolution" is quite important for specifying and comparing the performance of LMA type instruments.

3. Signal-to-Noise Ratio. The only signals of interest in nondestructive testing are flaw related signals. Signals that are not flaw related must be considered noise. In nondestructive wire rope inspection, the noise is primarily caused by the very inhomogeneous rope structure (test specimen noise). Structure related noise signals will be referred to as Intrinsic

Noise in the following. The intrinsic noise causes serious problems, and it makes test signals always very noisy. As compared to the intrinsic noise, noise caused by other sources (system noise) is relatively insignificant. One type of system noise is caused by the so-called "echo effect" which will be discussed below.

4. Penetration. The penetration of a transducer is measured by the ratio of the signal amplitude, caused by an internal flaw, to signal amplitude, caused by an identical surface flaw. This ratio is also called the Penetration Ratio in the following. Note that the penetration ratio depends on the geometry of the sense coil as well as the rope and flaw geometry.

5. Sensitivity. The sensitivity of a sensor is measured as the signal amplitude caused by a predetermined flaw. The sensitivity of a coil is primarily determined by the number of turns and by the coil geometry.

6. Repeatability. Many sensors used for rope inspection are either subdivided or are otherwise not rotationally symmetric. Hence noise as well as flaw signals depend on the azimuthal position of the rope with respect to the sense coil, and complete repeatability of signals cannot be assured.

In optimizing the above design criteria, only sensitivity causes no problems. Sensitivity can easily be increased by increasing the gain of the signal amplifiers and/or the number of turns of the sense coils.

The problems associated with signal-to-noise ratio, repeatability and penetration are somewhat related. They are discussed in the following.

In previous designs [2], we identified the subdivided and hinged sense coils together with the nonhomogeneous rope structure as the primary cause of intrinsic noise. A steel wire rope is an arrangement of separate wires wound in a helical shape to form strands. The strands are then laid together in a helix to form the rope. The strands cause a leakage flux field parallel to the strands as shown in Figure 7. The flux surrounding the rope has an axial component B_z and an azimuthal component B_φ. Since previous designs used subdivided search coils as in Figure 1, the azimuthal field component induced a noise voltage in the sense coil as the rope moved. We called this noise voltage "Intrinsic Noise" [2].

The amplitude of flaw related pulses depends on the location of the flaw within the rope (its eccentricity). The closer the flaw is to the sense coil, the higher is the corresponding flaw signal amplitude. Since the inhomogeneous rope surface, which is very close to the sense coils, primarily causes the intrinsic noise signal, the signal-to-noise ratio can become quite small. The intrinsic noise is superimposed on defect signals and can significantly distort the defect signals. The defect signals are used to estimate the defect parameters, and this can introduce errors in the flaw parameter estimate.

Furthermore, in previous designs the subdivided coils were not rotationally symmetric [2], [3]. Therefore, noise as well as flaw signals depended on the azimuthal position of the rope with respect to the sense coils, and complete repeatability of signals could not be assured.

To remedy this situation, we used subdivided sense coils with iron cores for the new instruments. Figure 6 shows a schematic of this new coil arrangement. Note that the iron core can have complete rotational symmetry without an air gap at the subdivision. The ferrous core guides the leakage flux through the coils. Therefore the sense coils enclose the total magnetic leakage flux. Because of its rotational symmetry, the coil is now completely insensitive to the azimuthal component of the leakage field. Therefore an improved signal-to-noise ratio was achieved. Furthermore, since the coil is rotationally symmetric, we have eliminated the influence of the angular defect position on the test signal, with an improved repeatability of the test signal. The basic coil performance was not changed by the insertion of ferrous cores. Hence, most conclusions of this report hold equally well for air and ferrous cores.

The coils shown in Figures 5 and 6 have a relatively complicated shape and their manufacture requires significant craftsmanship. Therefore, for smaller instruments, we chose a simpler coil design. Figure 8 shows the simplified design. Here the sense coils are wound directly on the permanent magnet yoke. Steel pole pieces channel the magnetic leakage flux through the permanent magnet yokes. The sense coils measure the changing magnetic flux in the yokes. The simplified design is much easier to manufacture and less expensive than the coils of Figure 6. However, since the simplified design is not rotationally symmetric, it has a slightly lower signal-to-noise ratio and signal amplitudes depend slightly on the angular position of the flaw with respect to the sense coils.

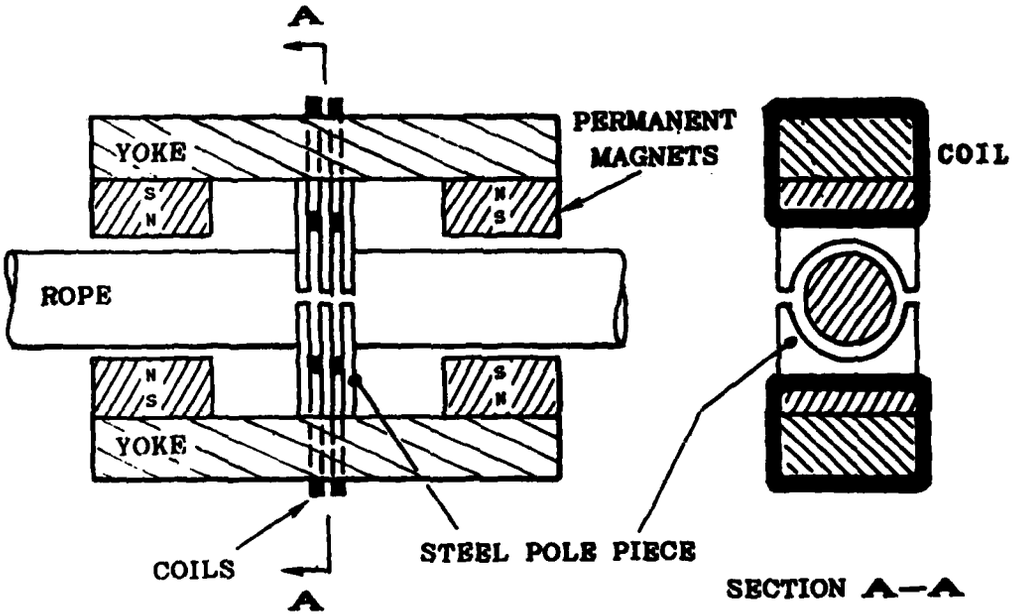

Figure 8: Simplified Sense Coils with Ferrous Core

The LMA trace shows continuous flaws and localized flaws, such as broken wires, with considerable accuracy. However, a differential sensor arrangement is better suited to highlight rapid flux changes caused by localized flaws such as broken wires. Therefore, a localized flaw (LF) signal of the differential type is highly desirable. In the early designs of the new LMA instruments, we used the time derivative of the LMA signal as the LF signal. This approach, however, makes the LF signal amplitudes proportional to speed. If the LF signal is to be used for a quantitative defect evaluation, obviously it must be speed independent. To make the LF signal independent of speed, we chose a differential coil arrangement as in Figures 8 and 9. In this configuration, two coils of the above design, spaced an incremental distance apart, are used. The two LMA signals from both coils are subtracted. The difference signal serves as the LF signal. It is easy to see that this difference signal is substantially the spatial derivative of the LMA signal. The spatial derivative of the LMA signal is independent of rope speed, as required.

The coils of the new design have an excellent resolution as compared to the LMA sensors of competing instruments. Figure 10 shows a performance comparison of one of the new prototype main flux instruments with a Canadian main flux instrument. Although the scales of both strip chart recordings are different, this figure shows the drastically improved resolution and quantitative resolution of the new instruments. The new instruments have a quantitative resolution of approximately 2 to 3 inches, depending on the design. In comparison, the quantitative resolution of other instruments is approximately 30 inches [24], [25].

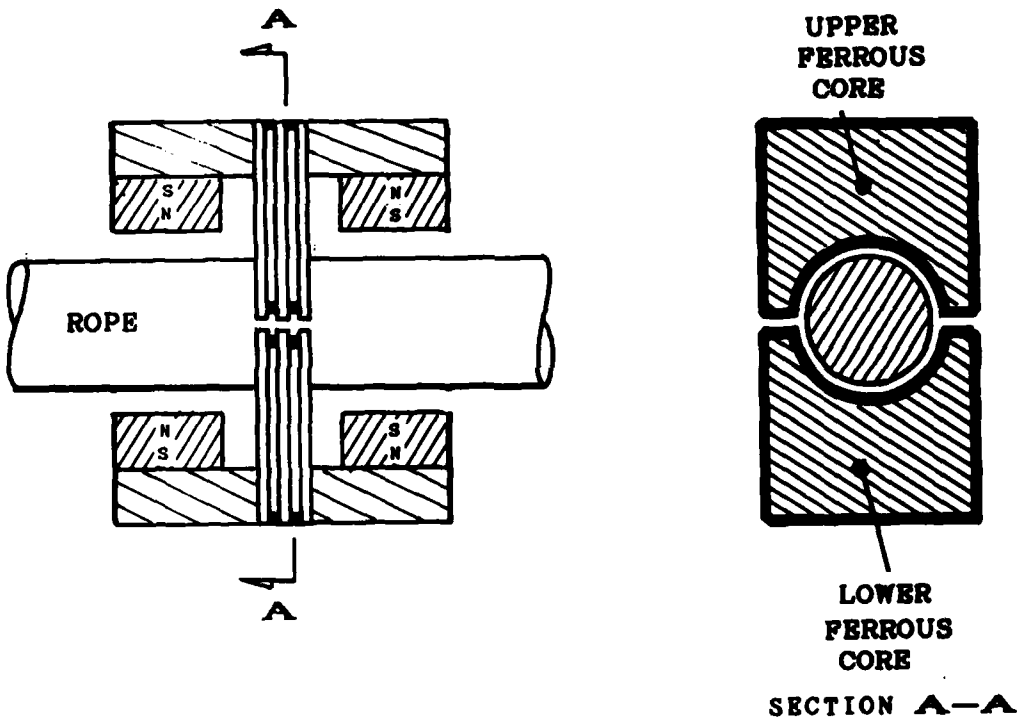

Figure 9: Double Coil Array

NEW PROTOTYPE LMA INSTRUMENT

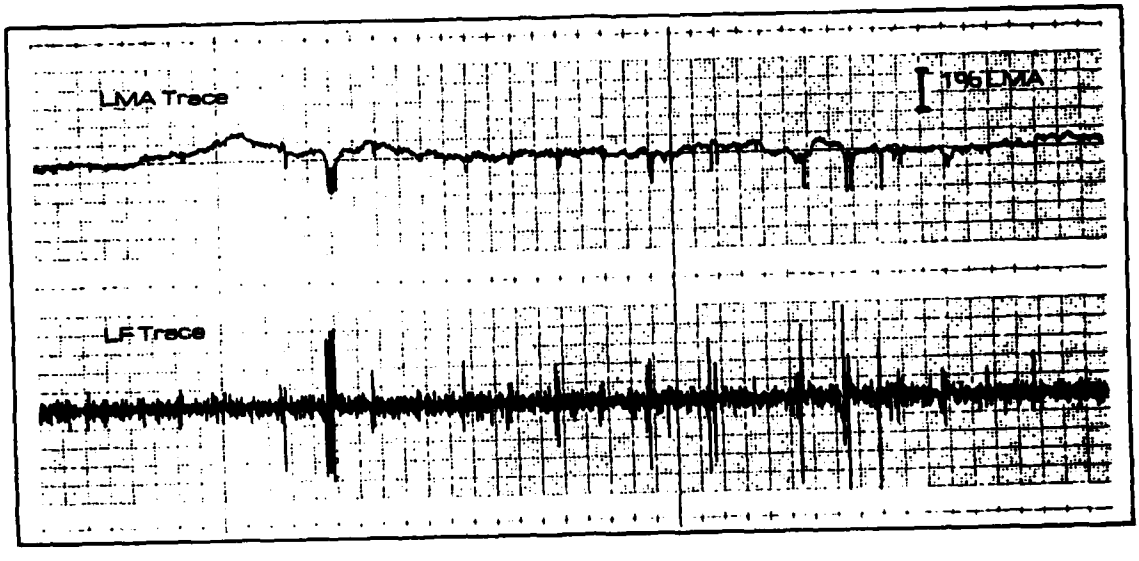

PREVIOUS STATE-OF-THE-ART INSTRUMENT

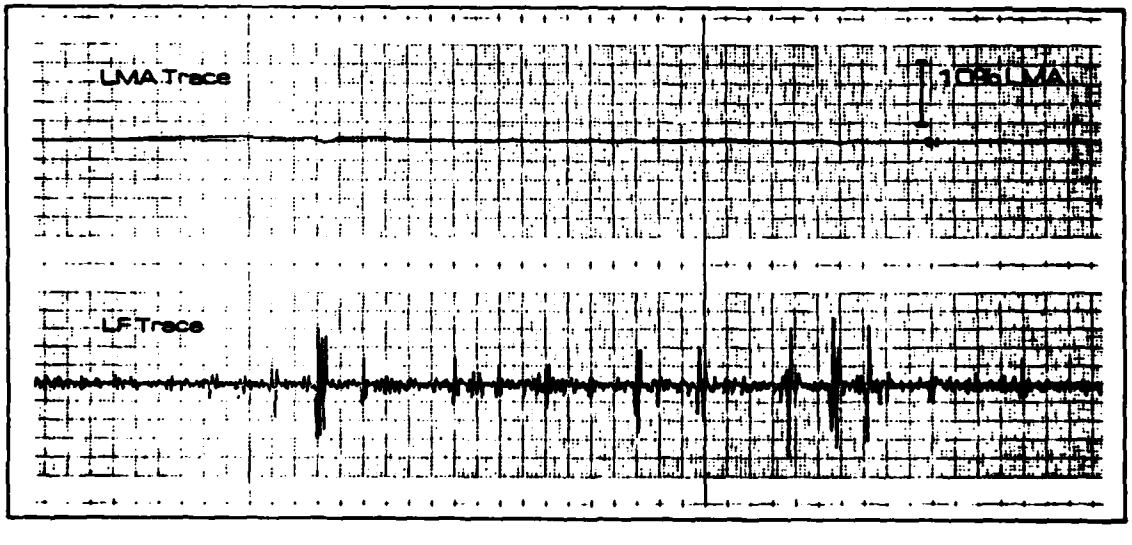

Figure 10: Performance Comparison of New Prototype LMA Instrument with Previous State-of-the-Art LMA Instrument

The following example illustrates the importance of a high quantitative resolving power. Consider a (hypothetical) rope with a 10% completely uniform loss of cross-sectional area extending over a length of 3 inches. An instrument with a quantitative resolution of 2 inches can determine the exact LMA caused by this flaw. However, an instrument with a quantitative resolution of 30 inches would indicate the same fault as a 1% loss of cross-sectional area extending over a length of 30 inches; a very inaccurate indication of the true rope condition. Of course, both instruments would give a correct indication of uniform faults extending over a length of 30 inches or longer.

High quantitative resolving power is important. This becomes evident by considering typical failure modes of ropes which show a significant loss of metallic cross-sectional area. In many naval and mining applications, high humidity causes condensation and accumulation of water inside the rope. The water causes corrosion. Therefore, most of these ropes, close to retirement, show advanced internal corrosion, often combined with internal interstrand wear. Usually this deterioration is not visible from the outside.

Corrosion causes typical patterns of metal loss: Corrosion pitting and corrosion patches. Pitting occurs in the form of very short localized losses on the surface of individual wires. Corrosion patches extend over a number of wires. They have a tendency to form groups with the length of patches extending over only a few inches. Often some of the wires within a patch have been completely separated by corrosion and form clusters of broken wires. To determine a rope's metal loss and loss of strength with reasonable accuracy, high quantitative resolution, of no more than a few

inches, of the test instrument is obviously important.

4. COMPUTER-AIDED QUANTITATIVE DEFECT IDENTIFICATION

The quantitative resolution of the LMA sense coils is approximately 50mm which is a considerable improvement as compared to the previous state of the art. The quantitative resolving power can be improved further by using a computer-aided quantitative defect identification method. One approach is discussed in the following.

The geometry of a defect in combination with the sensor geometry influences the shape of the defect signal in a very complicated fashion. The sense coils and rope flaws are characterized by the following geometrical parameters (see Figure 11):

Coil Radius: R

Coil Distance: d

Flaw Eccentricity: x

Flaw Length: l

Flaw Cross-Sectional Area: q

The following parameters characterize the defect signals (see Figure 11):

Peak LMA Signal Amplitude: LMA_P

Peak LF Signal Amplitude: LF_P

LF Signal Peak Distance: s

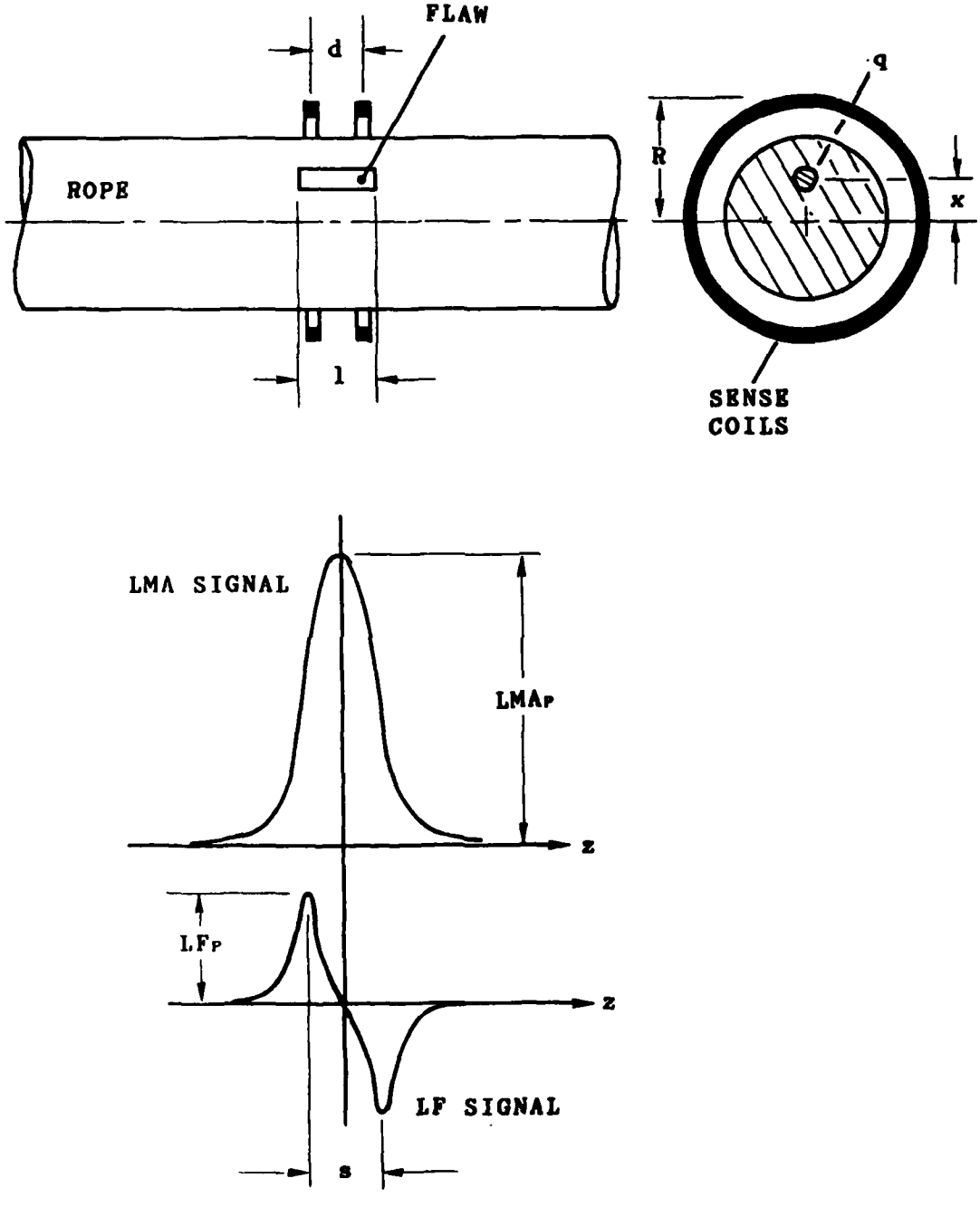

Figure 11: Defect, Coil and Rope Geometry, and Test Signal Parameters

From these signal parameters, we derive the following supplementary signal parameters:

Normal Flaw Cross-Sectional Area: q_N (Cross-Sectional Area of a Standard Calibration Wire)

Normal LMA Signal Amplitude: LMA_{PN} = LMA_P for a well defined standard surface flaw with infinite flaw length and cross-sectional area q_N (e.g. missing or added wire with known dimensions)

Normal LF Signal Amplitude: LF_{PN} = LF_P for a well defined standard surface flaw with infinite flaw length and cross-sectional area q_N (e.g. missing or added wire with known dimensions)

Signal Amplitude Ratio: $SAR = LF_P/LMA_P$

Normal Signal Amplitude Ratio: $SAR_N = LF_{PN}/LMA_{PN}$ (SAR of a surface flaw with infinite flaw length)

Relative Signal Amplitude Ratio: $SAR_R = SAR/SAR_N$

Relative LMA Signal Amplitude Ratio: $LMA_R = LMA_P/LMA_{PN}$

Relative LF Signal Amplitude Ratio: $LF_R = LF_P/LF_{PN}$

The above defined Normal (LF and LMA) Signal Amplitudes are easily determined by attaching a standard calibration wire with known dimensions (a "standard flaw") to the rope surface and by measuring and evaluating the corresponding flaw signal amplitudes. All other rope flaws are then evaluated relative to this standard flaw.

Any implementation of automatic defect characterization schemes using magnetic flux methods requires substantially four distinct signal processing steps [2]:

1. Test Signal Generation. Material inhomogeneities in the test specimen cause disturbances of the magnetic field. The changing magnetic field induces the test signals in the sensors.

2. Test Signal Conditioning. To make the test signals useful for the subsequent processing, they usually have to be modified. Pre-amplification is required. Filtering and/or non-linear signal modification are often necessary.

3. Signal Parameter Determination. From a practical viewpoint very few parameters are available to characterize flaw signals, either in the time domain or in the frequency domain. Characteristic parameters are flaw pulse-amplitude and pulsewidth or pulse distances (in the time domain) or signal amplitude and signal frequency (in the frequency domain). Because of the inevitable inaccuracies, caused by noise, a more detailed characterization of the test signals by more than the above parameters does not appear practical at the present time. The signal parameters are extracted from the test signals during this step.

4. Flaw Parameter Computation. The flaw geometry is computed from the signal parameters during this step.

The correspondence between signal parameters and flaw geometry is not unique, i.e. flaws of different shape and location can produce identical signals. To improve the estimate of the flaw geometry, the number of available independent signal parameters could be increased by utilizing an array of sensors. This approach was used in the Phase I study [2] where two concentric coils were used to produce two independent test signals.

The present approach uses a greatly improved sense coil arrangement which allows a direct and simple quantitative determination of a rope's metal loss for faults which are longer than approximately 2 inches. To evaluate shorter flaws, a slightly more involved quantitative defect identification approach is necessary. The use of concentric coils, as in [2], is not practical for the new sensor configuration. Therefore the fault signal (the LMA signal) and its spatial derivative (the LF signal) are used to derive a sufficient number of independent defect parameters. The above approach can then be used to implement a quantitative defect identification scheme. Figure 12 shows a functional block diagram of the implemented automatic defect characterization method.

The qualitative defect identification approach will now be explained in an exemplary fashion by using actual examples. The coil and flaw parameters for these examples are:

Coil Radius: R = 12.5 mm

Coil Distance: d = 5 mm

Flaw Eccentricity: x = 0 - 9.5 mm

Flaw Length: l = 5 - 80 mm

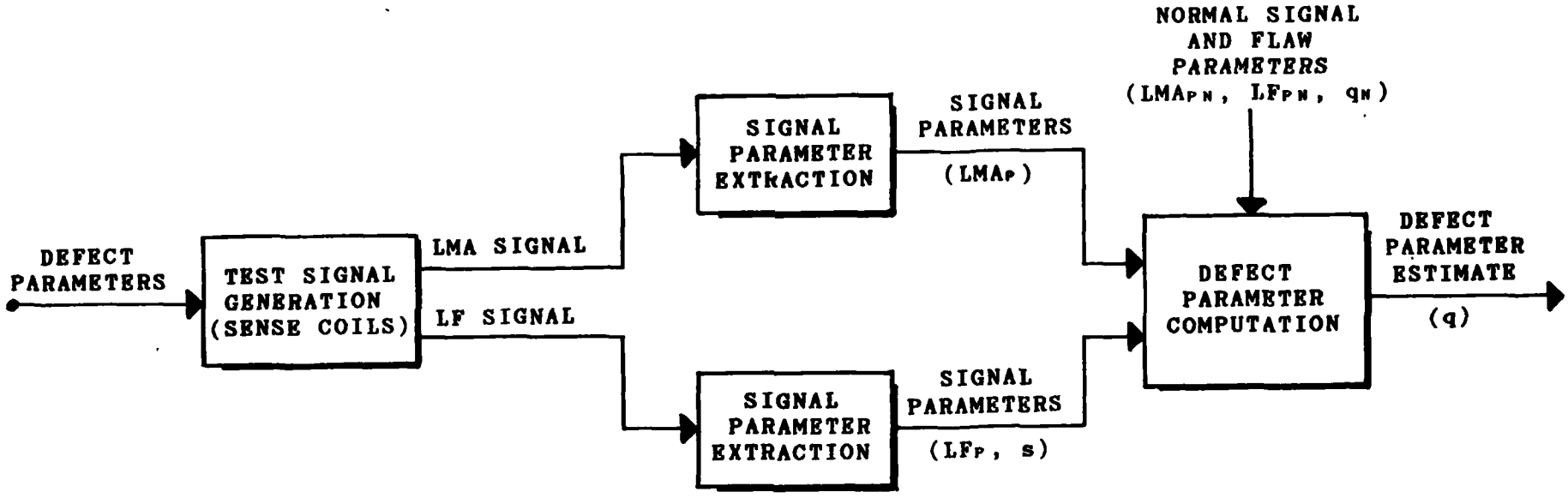

Figure 12: Functional Block Diagram of Defect Identification Scheme

To obtain the experimental test results, pieces of test wires were attached to the rope, simulating an increase of metallic cross-sectional area.

Figure 13 shows representative simulated waveshapes for a 3/4 inch (19 mm) diameter rope. Figure 14 shows corresponding actual flaw signals measured with one of the new main flux prototype instruments. Note the agreement between simulated and experimental results.

Figure 15 shows the flaw signal caused by a step change of metallic cross-sectional area which were obtained from a computer simulation [2]. Figure 16 shows the corresponding measured actual flaw signal. The area change in this case is caused by attaching an 18 inch long piece of wire to the rope. Step changes of metallic cross-sectional area will be called fundamental flaws in the following.

It is easy to see, that faults with any gap lengths l can be represented by linear superposition of the fundamental flaws and their corresponding flaw signals. Figure 13 shows simulated signals for flaws with different gap widths l and eccentricities x which were obtained from the elementary flaw signals by linear superposition. The results shown in Figure 13 illustrate how the amplitudes of the LMA signals decrease as the gap width of flaws decreases. For flaw lengths shorter than the quantitative resolution, the LMA signal does not indicate the complete metallic area loss.

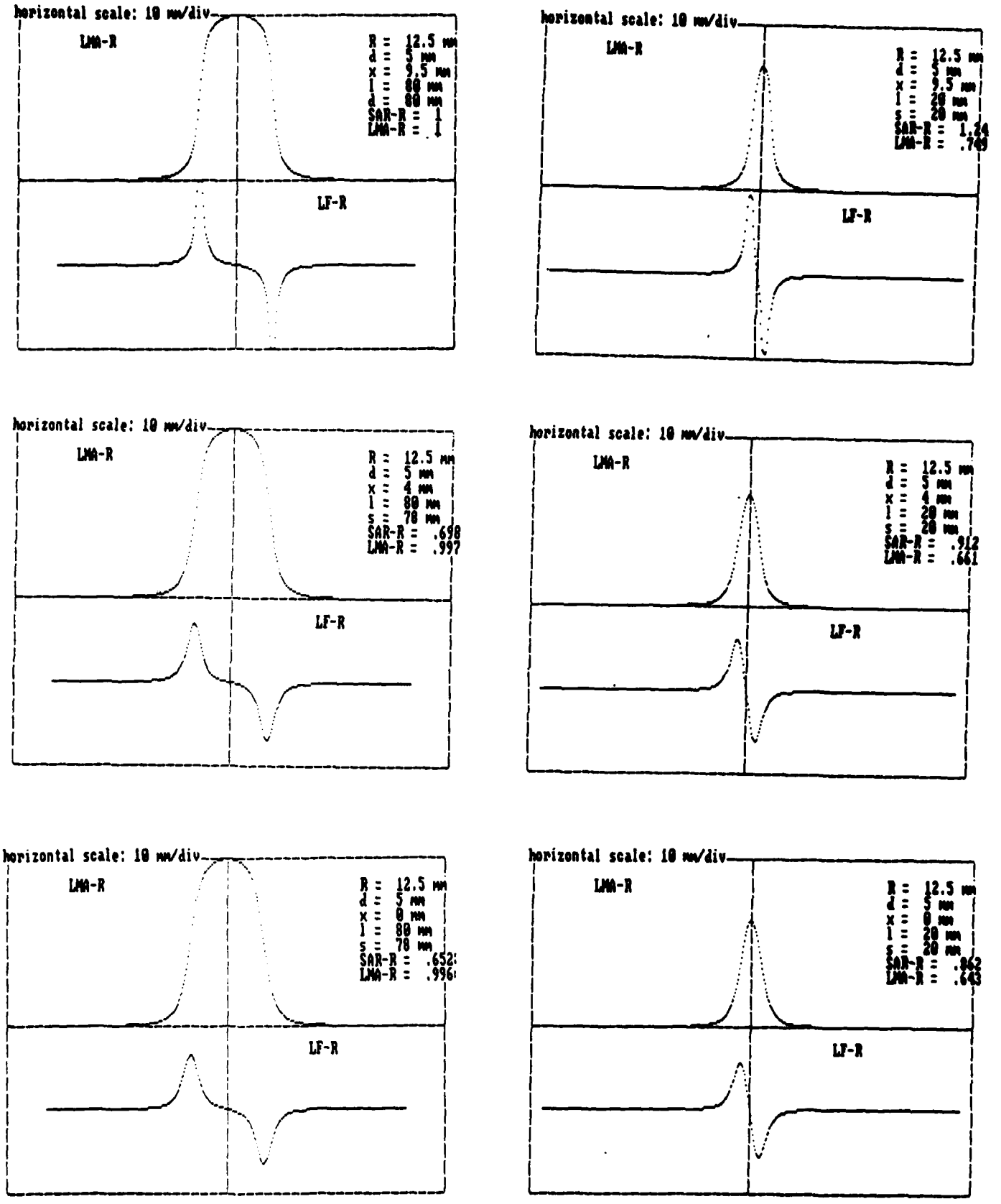

Figure 13: Defect Catalog of (Simulated) LMA and LF Defect Signals

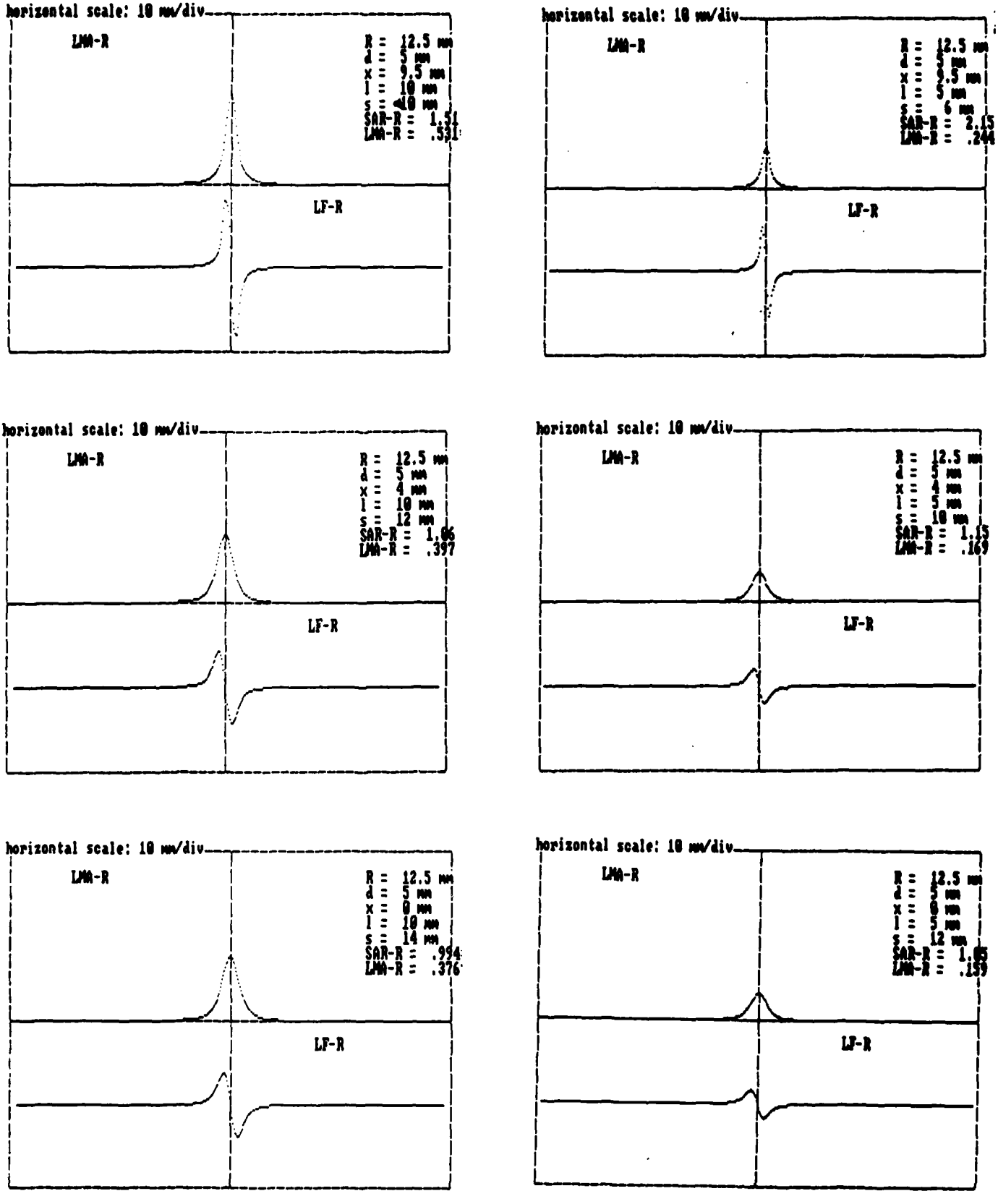

Figure 13: continued

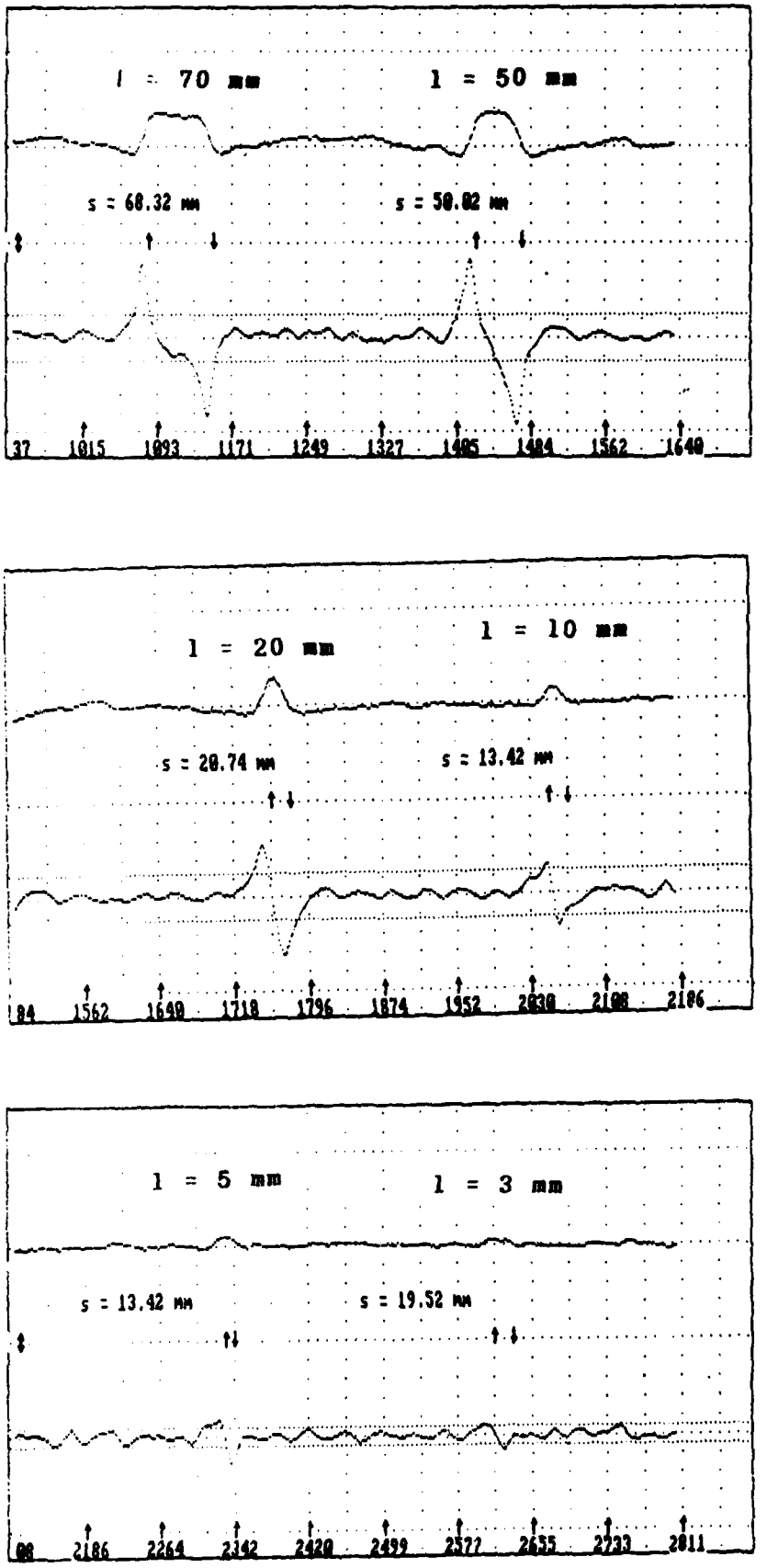

Figure 14: Measured Defect Signals

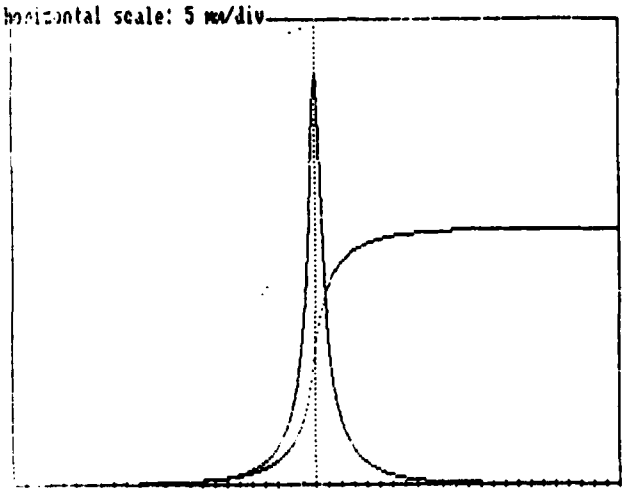

Figure 15: Simulated LMA and LF Signals For a Step Change of Metallic Area

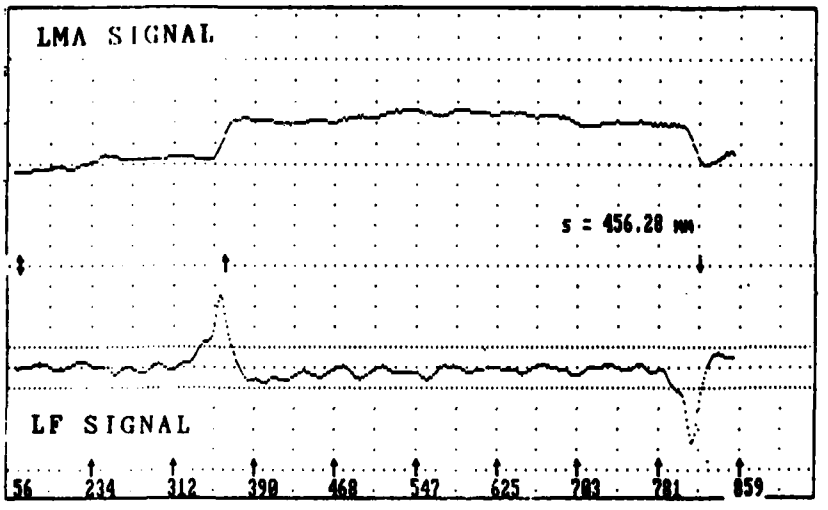

Figure 16: LMA and LF Signals for a Step Change of Metallic Area (Experimental Results)

Figure 17 shows the measured metallic area loss q_M as a percentage of actual metallic area loss q as a function of gap length l. This functional relationship can be approximated by

$$q_M/q = 1-\exp(-l/L) \qquad \{1\}$$

where L is a flaw distance constant. This approximate relationship {1} with L = 18mm is also indicated in Figure 17.

The actual area loss q as a function of measured area loss and flaw length can then be approximated by the following expression

$$q/q_N = (LMA_P/LMA_{PN})/(1-\exp(-l/L)) \qquad \{2\}$$

To calibrate the instrument for each rope, the normalized values LMA_{PN} and LF_{PN} are determined by attaching a wire of known cross sectional area q_N to the rope and by recording the corresponding LMA and LF signals. All flaws can then be quantitatively evaluated with respect to this reference wire.

To implement a quantitative defect identification scheme, we consider Figures 13 thru 17. We observe that, for flaws longer than approximately 15mm, the flaw length l is approximately equal to the peak-to-peak distance s of the LF signal. Using Figure 18, it is then simple to determine the actual flaw length l from the peak-to-peak distance s.

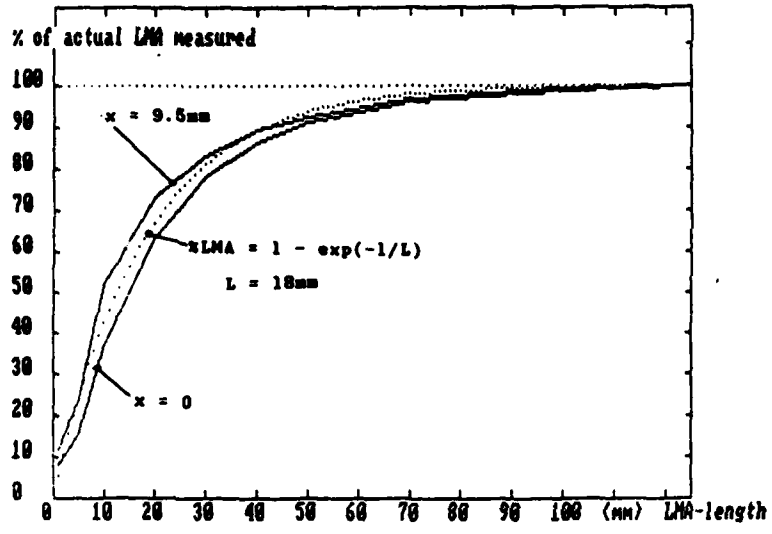

Figure 17: Measured Metallic Area Loss as a Percentage of Actual Metallic Area Loss

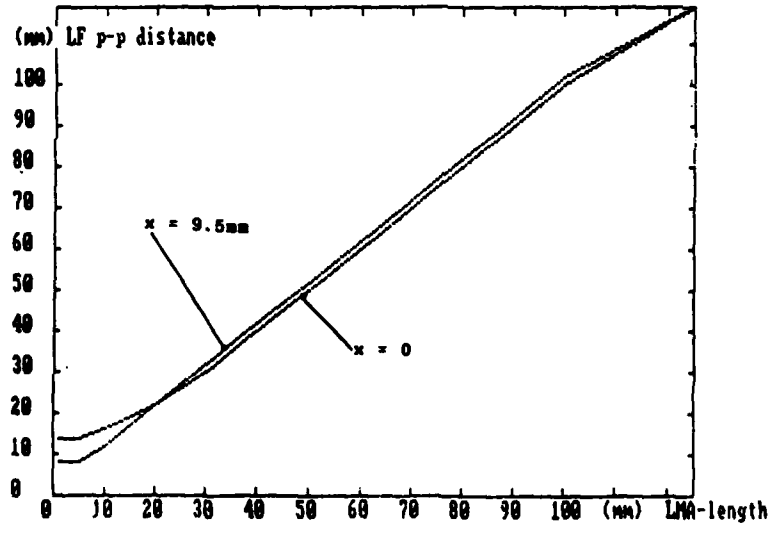

Figure 18: LMA Gap Length as a Function of LF Peak-to-Peak Distance

As illustrated by Figures 18, 13 and 14, the determination of flaw length becomes more complicated for shorter flaws. In this case, the peak-to-peak distance s is no longer a good indication of flaw length l. However, using Figure 19, the Relative Signal Amplitude Ratio SAR_R can be used to derive at least an estimate of l. Note that, for short flaws, the accuracy of the flaw length estimate is reduced further because of the inherent difficulty in establishing the flaw length for short flaws combined with the usually low signal-to-noise ratio caused by the inevitable intrinsic noise.

After we have determined the flaw length l, we use Figure 17 or Equation {2} to determine the actual loss-of-metallic-area. The quantitative defect identification is now complete.

A closer examination of Figures 13 thru 20 reveals a few features of the new sense coils which we will discuss in the following.

Since the intrinsic noise signal is primarily caused by the inhomogeneous rope surface, it can cover up signals caused by interior flaws to such an extent that they can no longer be detected. As discussed in [2], because of this, the penetration ratio has to be maximized for an optimum signal-to-noise ratio. The penetration ratio was defined above.

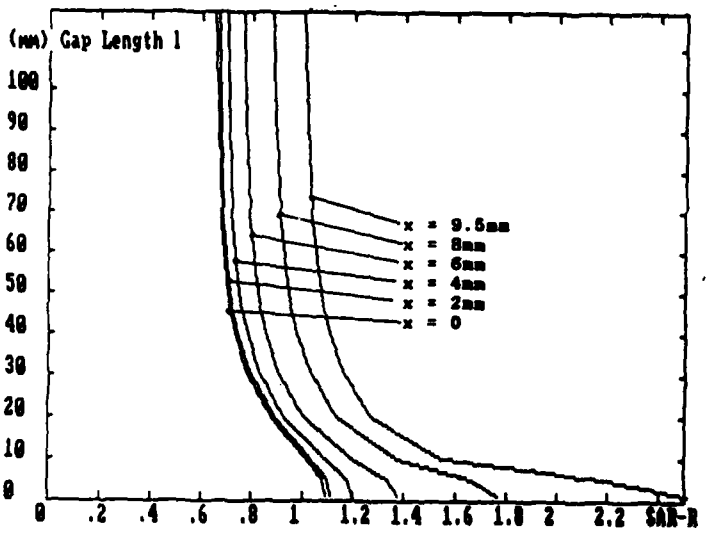

Figure 19: LMA Gap Length as a Function of Relative Signal Amplitude Ratio and Eccentricity

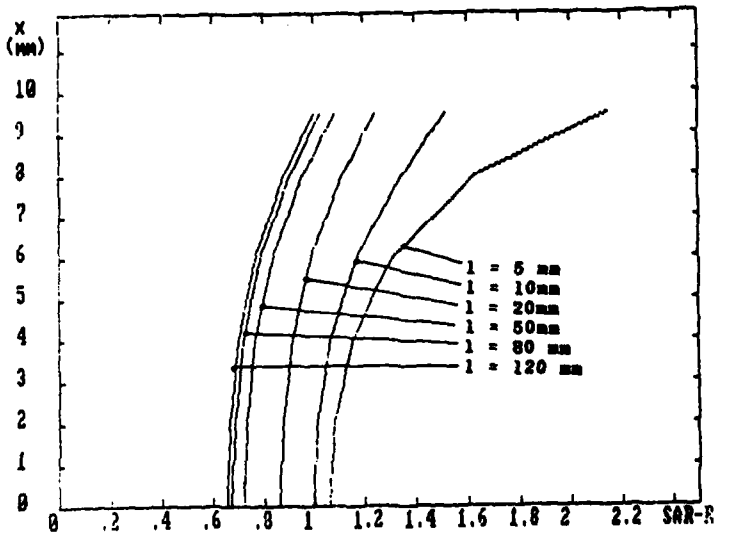

Figure 20: Eccentricity as a Function of Relative Signal Amplitude Ratio

For short flaws, with gap widths less than 5 mm and a 3/4 inch rope, the present sensor has a penetration ratio of .72 for the LMA signal and a penetration ratio of .49 for the LF signal. This compares with penetration ratios of .22 and .40 for the comparable double-differential coils which were previously used for the Phase I research. Note that for gap widths longer than approximately 2 inches the penetration ratio for the LMA signal for the new coils is close to 1.

This implies that, because of the higher penetration ratios, the new coils offer a significantly improved signal-to-noise ratio as compared to the previous double-differential coils [2]. Furthermore, the new coils have a considerably improved capability of detecting internal flaws. These observations are borne out by the experimental results.

On the other hand, these high penetration ratios indicate that, for the new sense coils, the flaw signal amplitudes are not very dependent on the flaw eccentricity x. This insensitivity, combined with inaccuracies caused by the intrinsic noise, makes a quantitative determination of the location of the flaw within the rope cross section impossible from a practical point of view. Figure 20, which shows the flaw eccentricity x as a function of the Normalized Signal Amplitude Ratio SAR_N and Flaw Length l illustrates this observation.

The quantitative determination of flaw eccentricity would undoubtedly be a desirable feature. Therefore alternative methods for a determination of the flaw location will be investigated. Any new approach should, however, retain the excellent performance characteristics of the present sensors.

5. ROPE MAGNETIZATION AND RE-MAGNETIZATION

Magnetic flux patterns within the rope and the sense head are very complex. This, under certain conditions, causes the new instruments to behave in a fashion which is not immediately obvious. One such peculiar behavior could be called the "Remagnetization Effect". The exact mechanism of the Remagnetization Effect is still not completely understood. We conducted a substantial number of experiments to investigate this phenomenon. The most plausible explanation is presented in the following.

Consider the strip chart recording of Figure 21. To make this recording, the test rope was first completely demagnetized. The instrument was then mounted on the rope at Position 1 on the recording, and the integrator was reset. As the steel rope moves through the sense head, the strong permanent magnets in the sense head permanently magnetize the rope. The presence of remanent residual magnetic flux in the rope causes a redistribution of the flux pattern within the rope and the sense head. As the rope moves, the changing permanent residual flux causes additional increasing magnetic flux inside the instrument which, for the first two or three feet of rope movement, induces an additional voltage in the sense coils. The previously zeroed LMA signal accordingly shows an increase as in Position 1 of Figure 21. This means, the redistributed flux causes an offset of the zero setting of the LMA signal which compromises the readings of the LMA channel if not properly accounted for.

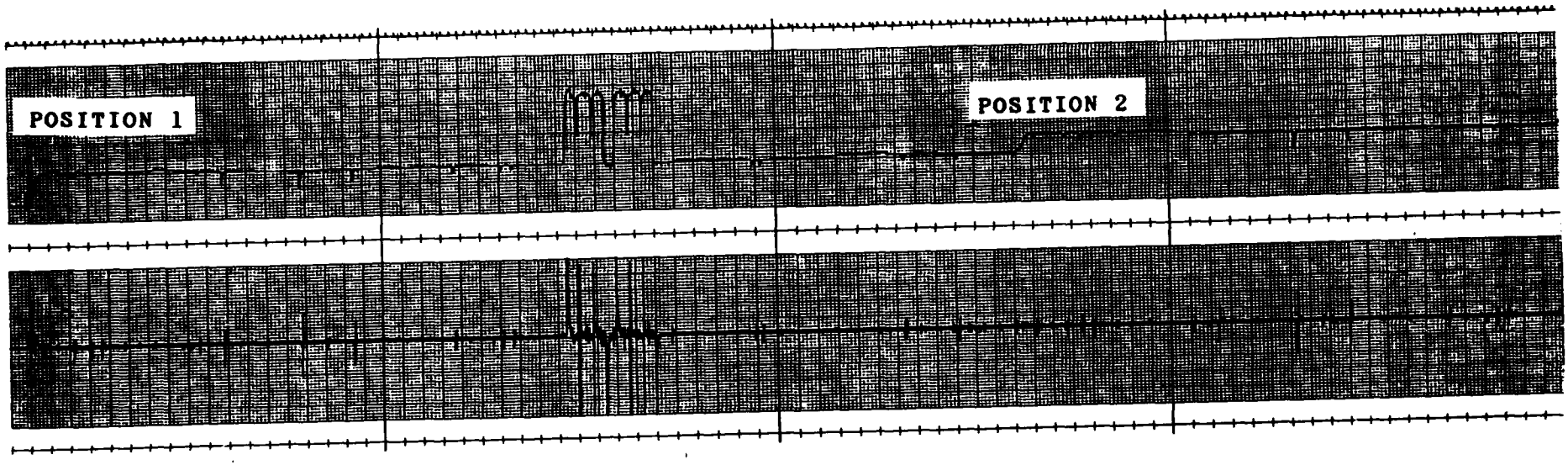

Figure 21: Remagnetization Effect

Now consider Position 2 of Figure 21. The test rope is spliced and forms a loop. (The splice is clearly visible in the chart recording). Because the rope forms a loop, Positions 1 and 2 are geometrically identical on the rope. Note that, if the instrument is located between Position 1 and Position 2 on the rope during the first circulation of the loop, that section of the rope which enters the instrument is unmagnetized, and the section of rope which leaves the instrument becomes permanently magnetized. Therefore during the first circulation, the magnetic state of the rope changes from "unmagnetized" before Position 2 to "permanently magnetized" after Position 2. As Position 2 on the rope approaches the instrument, the changing magnetic state of the the rope again influences the magnetic flux in the instrument. This, as previously in Position 1, causes another rise of the LMA signal at Position 2 on the chart. After the first complete circulation of the loop, the rope is magnetically homogenized and no further offsets of the LMA trace occur.

This "Remagnetization Effect" is explained further in the following.

Assume the sense head is mounted on a completely demagnetized rope. Now the rope moves a short distance. That part of the rope which leaves the instrument becomes permanently magnetized and retains a residual flux density in the direction of the rope axis. Consider the magnetic flux in the rope and the magnet assembly as shown in Figure 22. In the figure, we assume that the instrument has moved from position A to B. Figure 22 also shows a sketch of the axial flux density B_z. Note the magnetic reversal zone under the pole pieces where the magnetic flux changes directions. Over the distance A-B the rope is now permanently magnetized with residual

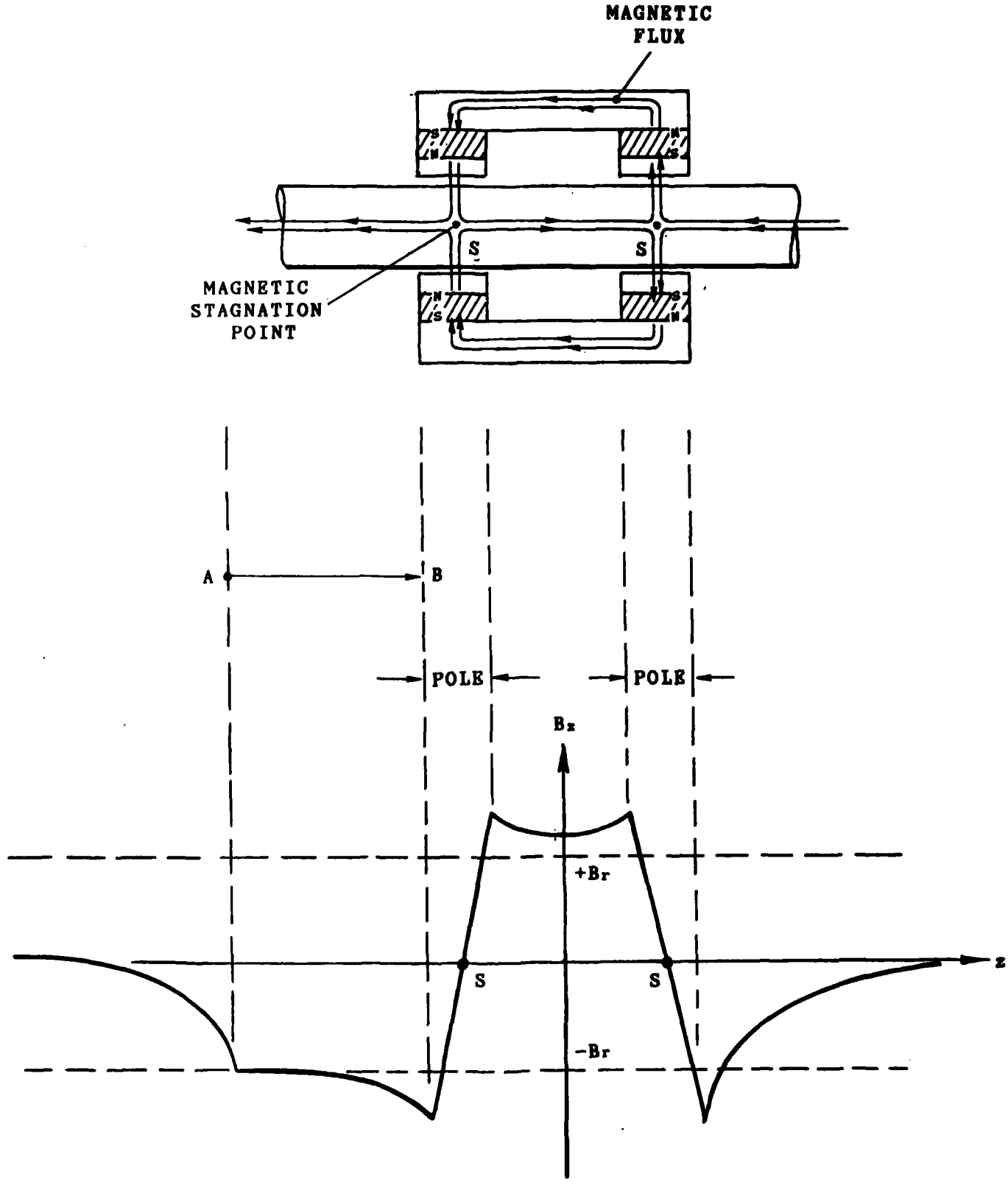

Figure 22: Magnetic Flux in Magnetizer and Rope

flux density B_r. B_r causes an additional residual flux ϕ_r whose path in the instrument will now be traced.

Figure 23 shows a schematic of the magnetic flux pattern in the rope and in the sense head. Note that only that part ϕ_r of the magnetic flux is shown which is caused by the permanently magnetized rope section A-B. The rope between the magnetic poles is saturated and represents a high reluctance magnetic path for ϕ_r. The yoke is not saturated and represents a low reluctance magnetic path. Therefore a major portion of ϕ_r returns through the yoke, as indicated. The increasing residual flux ϕ_r causes a rise of the LMA signal, simulating an increase in metallic cross-sectional area. This becomes obvious by considering the leakage flux ϕ_l which would be caused by a decrease of metallic cross-sectional area. ϕ_l and ϕ_r have opposite directions. Therefore, ϕ_r is recorded as, and simulates, an increase of metallic area.

This explanation of the remagnetization effect suggests a solution of the problem. The effects of remagnetization can be reduced by increasing the incremental reluctance of the yoke. We conducted several, fairly involved experiments to verify this hypothesis.

The experiments showed that a simple reduction of the yoke's cross-sectional area is not feasible. This approach drives the magnet assembly into saturation and increases the incremental reluctance of the yoke, as postulated. However, by the same token, it increases the reluctance of the magnetic circuit and keeps the rope out of saturation. This, in turn, reduces the LMA signal amplitudes and decreases the measurement accuracy.

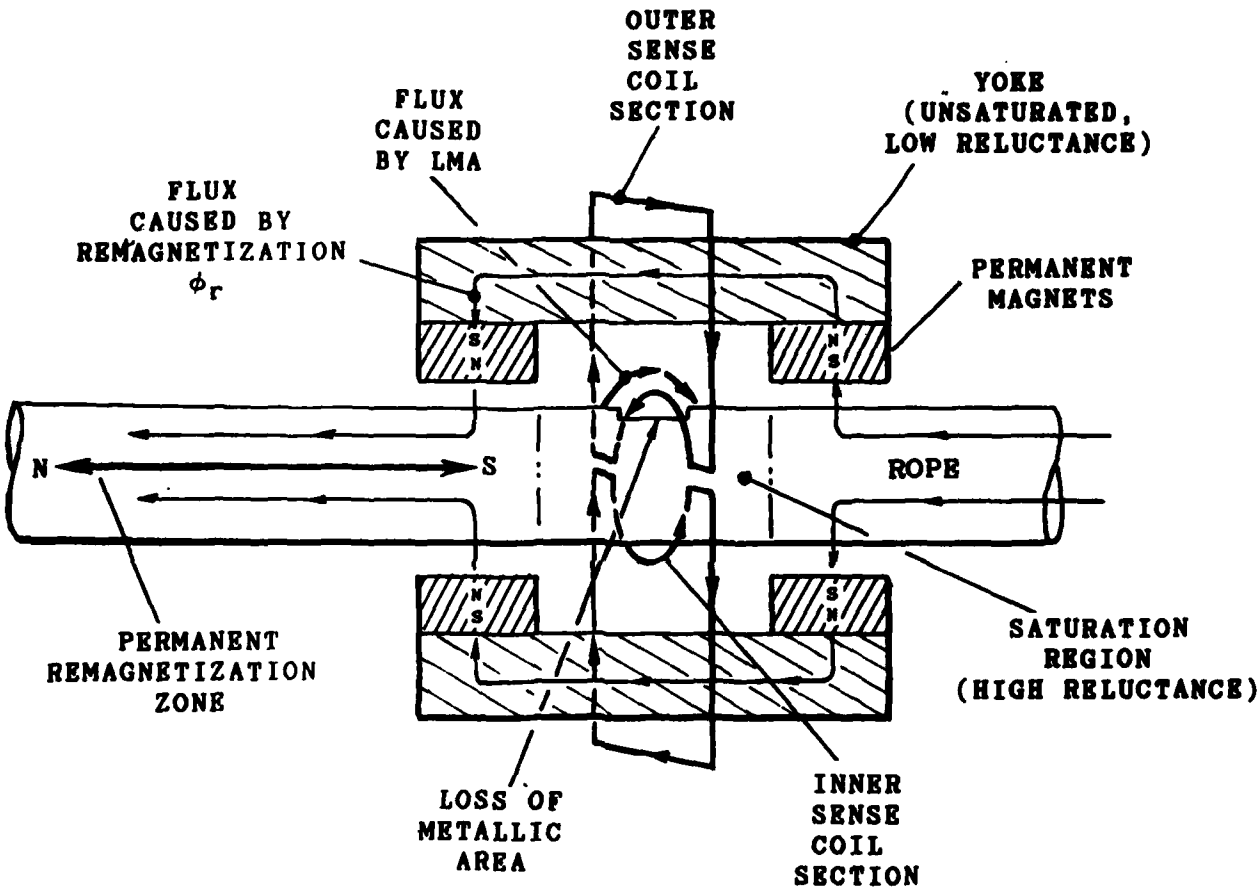

Figure 23: Magnetic Flux Caused by Re-Magnetization

An increase of the magnetic field, by adding permanent magnets, drives both, the yoke and rope, into saturation and increases the incremental reluctance of the yoke. Experiments show that this method is indeed feasible. It is presently being used for the design of additional prototype instruments. An increase of the number of permanent magnets can significantly reduce the effects of remagnetization.

Note that the problems caused by the remagnetization effect can be bypassed by magnetically homogenizing the rope before the inspection. The rope is homogenized by simply moving it through the instrument over its entire length. After the homogenization, the integrator voltage is reset to zero and the rope is inspected in the usual fashion. This procedure completely eliminates the effects of remagnetization. Magnetic homogenization of the rope, before the inspection, is a good practice. If feasible, the rope under test should be homogenized before the inspection.

Note that the LF signal is not affected by remagnetization. This signal is derived by subtracting the two signals from the differential coil arrangement shown in Figure 8. Therefore the effects caused by rope remagnetization are subtracted and cancel.

6. ECHO EFFECT

One peculiar behavior of the new instruments is the so-called "echo effect". This phenomenon is illustrated by the strip chart recording of Figure 24. A small replica (an "echo") of the actual flaw signal appears immediately before and after the actual flaw signal. The amplitude of the echo signal is less than 20% of the flaw signal and contributes to the

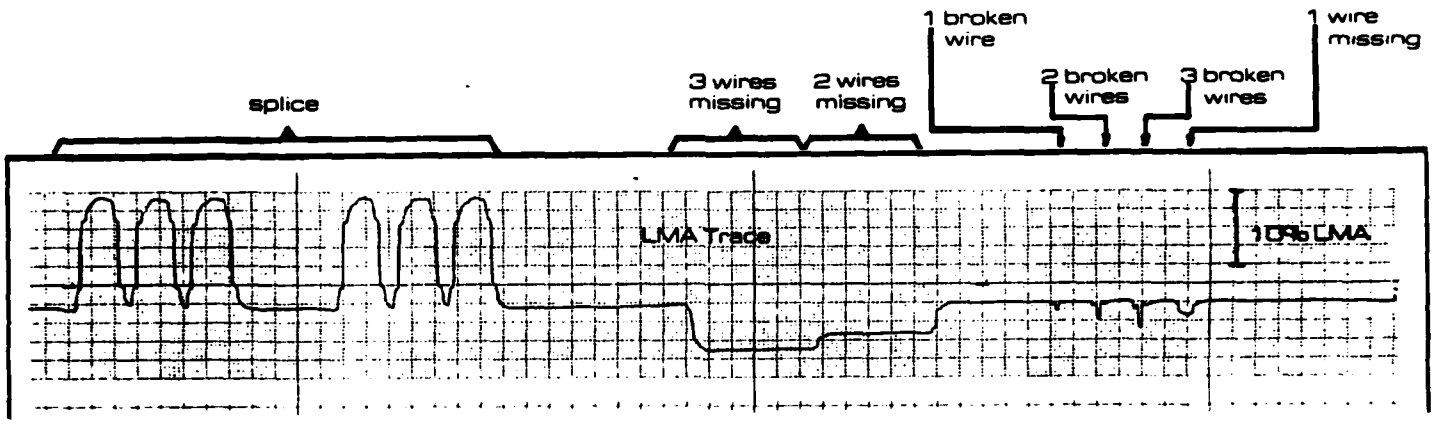

Figure 24: Echo Effect

intrinsic noise. While the signal-to-noise ratio of the new instrument compares very favorably with the signal-to-noise ratio of other instruments, elimination of the echo effect would undoubtedly improve the performance.

For an explanation of the phenomenon we first consider the magnetic field within the rope and the magnet assembly. Figure 25 shows the magnetic flux in the instrument. In particular, note the magnetic reversal zone under the pole pieces where the magnetic flux changes directions. Figure 25 also shows a sketch of the axial flux density B_z for a completely homogenized rope. The axial flux density within the rope changes its direction twice as the rope moves through the magnet. Outside the magnet, the direction of the axial flux density is opposite to the direction of the flux density inside the magnet. A permanently magnetized and homogenized rope regains its residual flux density after moving through the magnet.

Without changing any signals, t outer part of the sense coils could now be replaced by the (hypothetica equivalent coils indicated by dotted lines in the figure. This is plaus e because the outer coils can be moved to the position of the equiva t coils substantially without cutting any flux lines, i.e., without inducing any additional voltages in these coils.

The rope is magnetized inside and outside the magnetizer assembly, as in Figure 25, and any rope flaw causes a distortion of the magnetic flux. Therefore, upon approaching the instrument, any irregularity in the rope

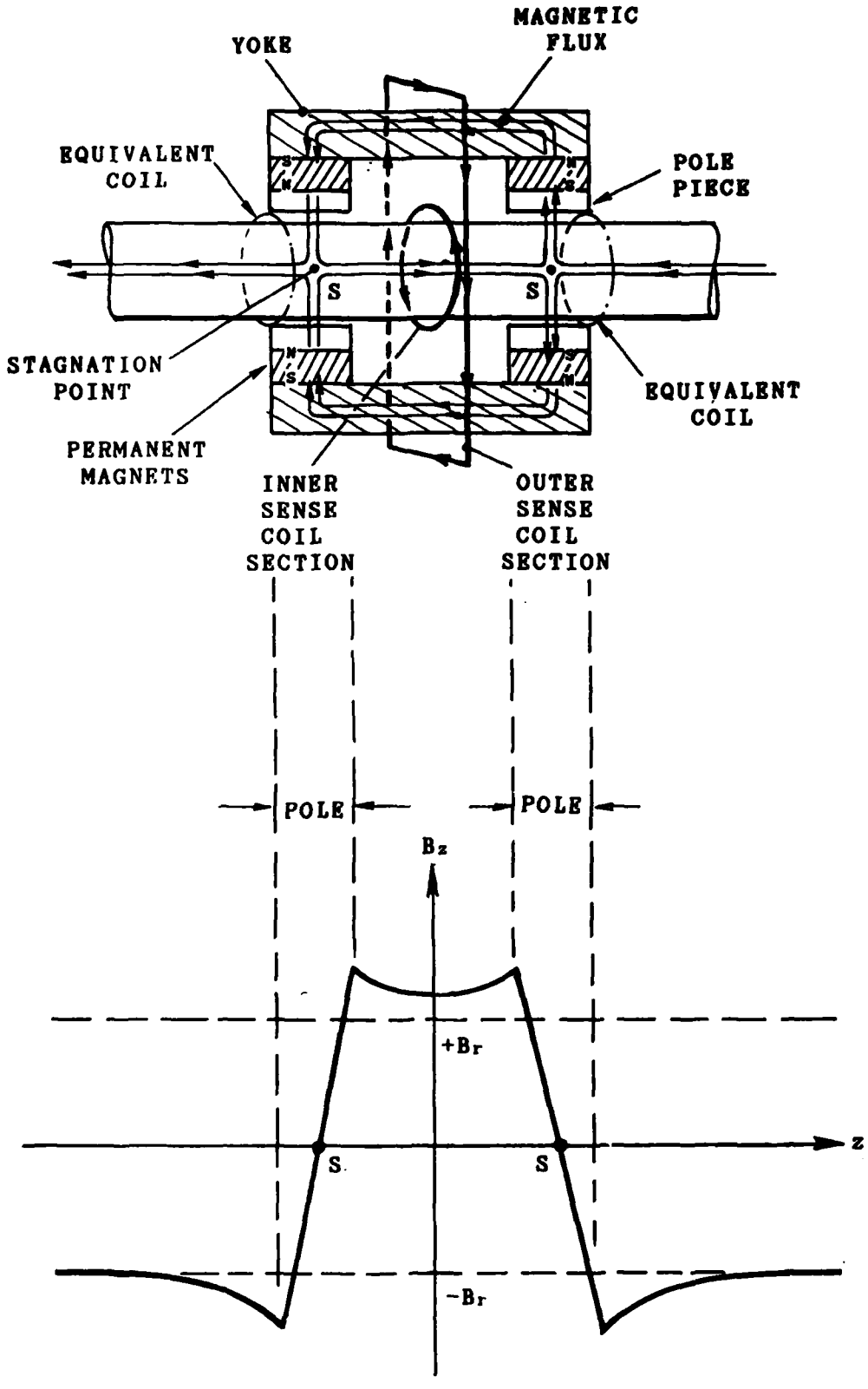

Figure 25: Echo Effect: Magnetic Flux Patterns

is first sensed by the outer part of the sense coils (or, according to the above discussion, by the equivalent coils). This causes the first "echo". The discontinuity is then sensed by by the inner part of the sense coil which gives the actual flaw signal. The outer part of the sense coil senses the discontinuity again while it moves away from the instrument. This causes the second "echo". Note that the magnetic flux density inside and outside the magnet and the coil orientations are such that the LMA signal and its two echoes have the same polarity.

Based on these findings, we modified the coil simulation program, considering the above described axial flux density in the rope together with the voltages induced in the outer sense coil. The simulated LMA signal of a step change of metallic area and the corresponding experimental signal are shown in Figure 26. Note the agreement between simulation and the experimental results.

Encouraged by computer simulation results, we made several attempts at eliminating the echo effect by placing the outer return coils into a magnetically neutral zone (the magnetic reversal zone in Figure 25). Figure 27 shows this arrangement. In this case, the magnet assembly was split into two pieces and the outer return coil was placed into the magnetically neutral zone between the two magnetizer pieces as shown in the figure. While the experimental results were consistent with the simulated results, the signals became very noisy. This noise is probably caused by the rapid reversal of the magnetic flux in the magnetically neutral reversal zone. Because of the inhomogeneous rope structure, the flux reversal area moves slightly back and forth in a random fashion. This

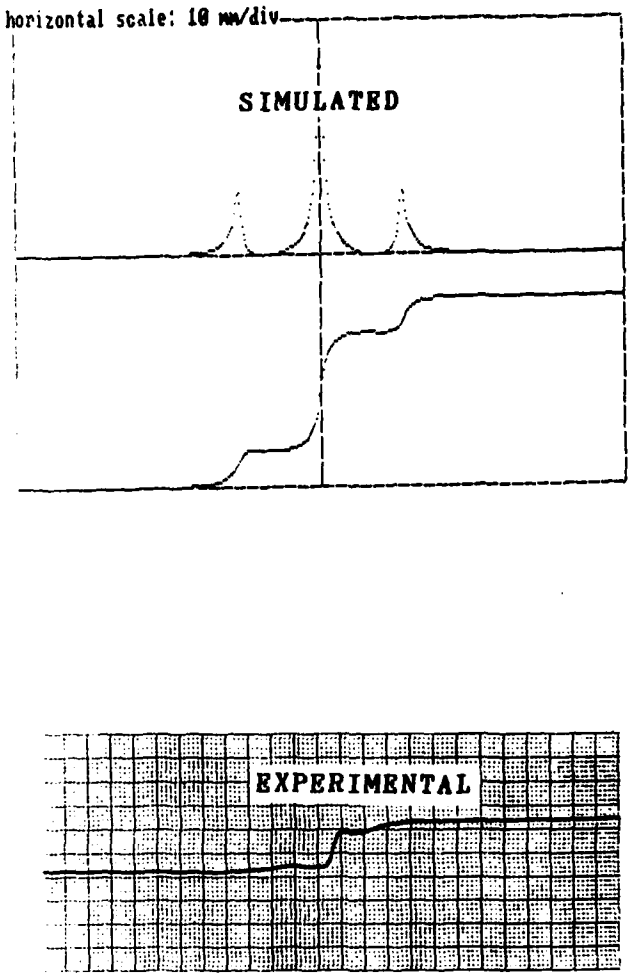

Figure 26: Echo Effect: LMA Step Response: Simulated and Experimental Results

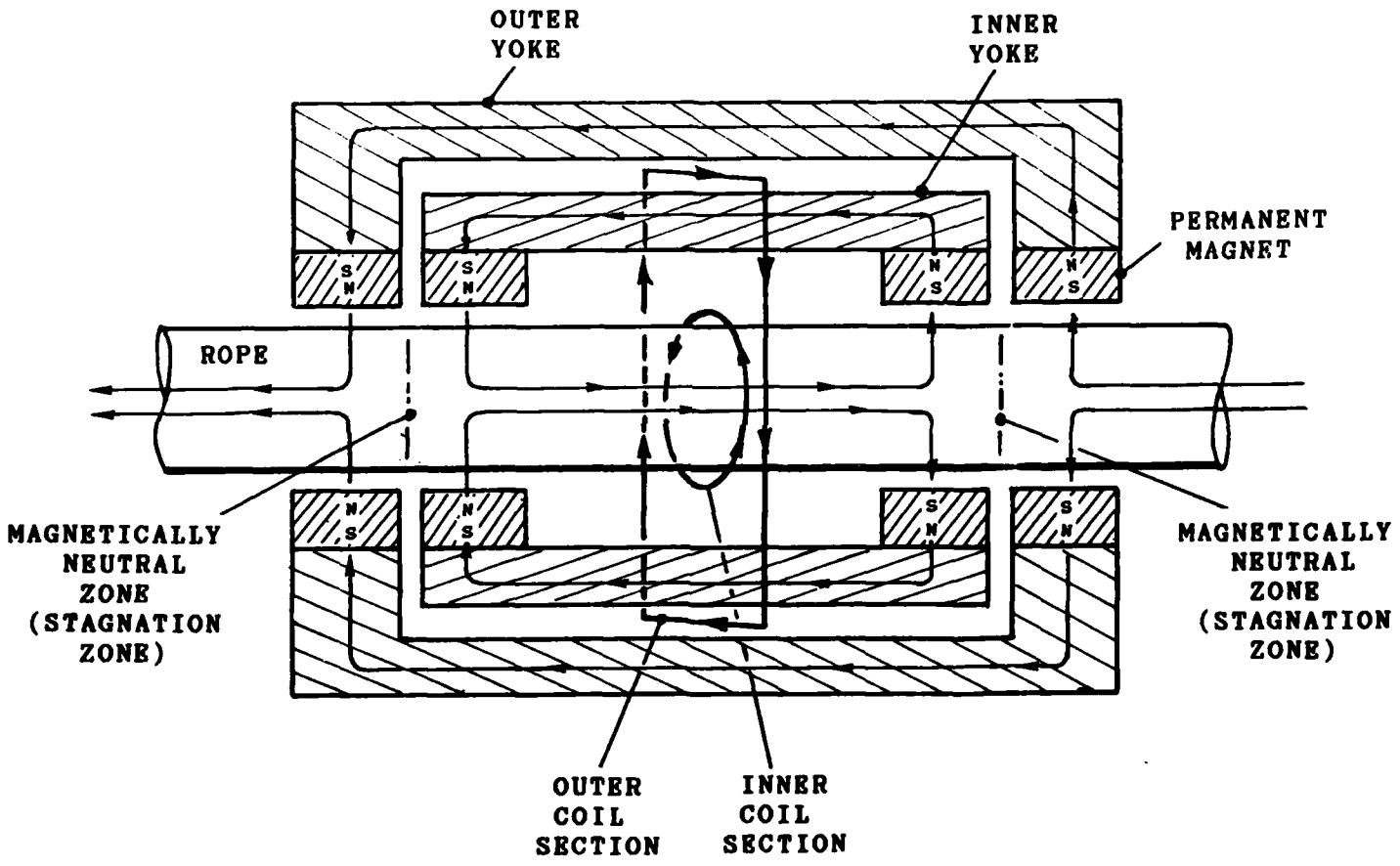

Figure 27: Split Pole Arrangement

movement induces additional noise voltages in the outer part of the sense coils. Therefore, we did not pursue this approach any further.

As stated above, the new instruments have a significantly better LMA signal-to-noise ratio and resolution than other instruments. Therefore we decided to postpone any further attempts to reduce the echo effect.

Note that the LF signal does not show an echo effect. This signal is derived from the differential coil arrangement of Figure 9. Therefore the echoes in the LF signal cancel.

7. INSTRUMENT FOR THE INSPECTION OF WIRE ROPE END SECTIONS

During operations, moving and standing wire ropes are subjected to, sometimes severe, vibrations which cause longitudinal and lateral rope oscillations. For all rope oscillation modes, longitudinal and lateral, rope terminations constitute oscillation nodes.

Hence, rope oscillations induce considerable bending and longitudinal stresses at the rope terminations which cause the wires to fatigue and eventually to break. Rope breakage at the terminations is one of the more common failure modes. This makes rope terminations one of the critical areas in assessing the rope condition.

Previously, none of the available NDI instruments were useful for inspecting rope end sections. This is due to four problems:

- Most instruments require a minimum rope speed which precludes the application of the instrument close to the rope termination.

- The signal amplitudes of most presently available instruments are speed dependent. Therefore it is very difficult to evaluate and compare results.

- The physical layout of all presently available instruments prevents a close approach of the sensor to the rope termination point.

- The magnetic flux at the rope termination becomes seriously distorted by the rope socket. Therefore it becomes very difficult to detect small flux perturbations caused by rope flaws in the distorted flux pattern.

The present design approach remedies most of the above shortcomings of existing instruments. An auxiliary set of coils is used which can be attached to regular instruments of the above described LMA type instruments. The auxiliary coils allow an LF inspection of the rope up to the rope termination socket. An LMA inspection, with reduced accuracy as compared to the regular LMA inspection, is also possible.

The physical layout of the new arrangement is sketched in Figure 28. The test arrangement substantially consists of two separate parts:

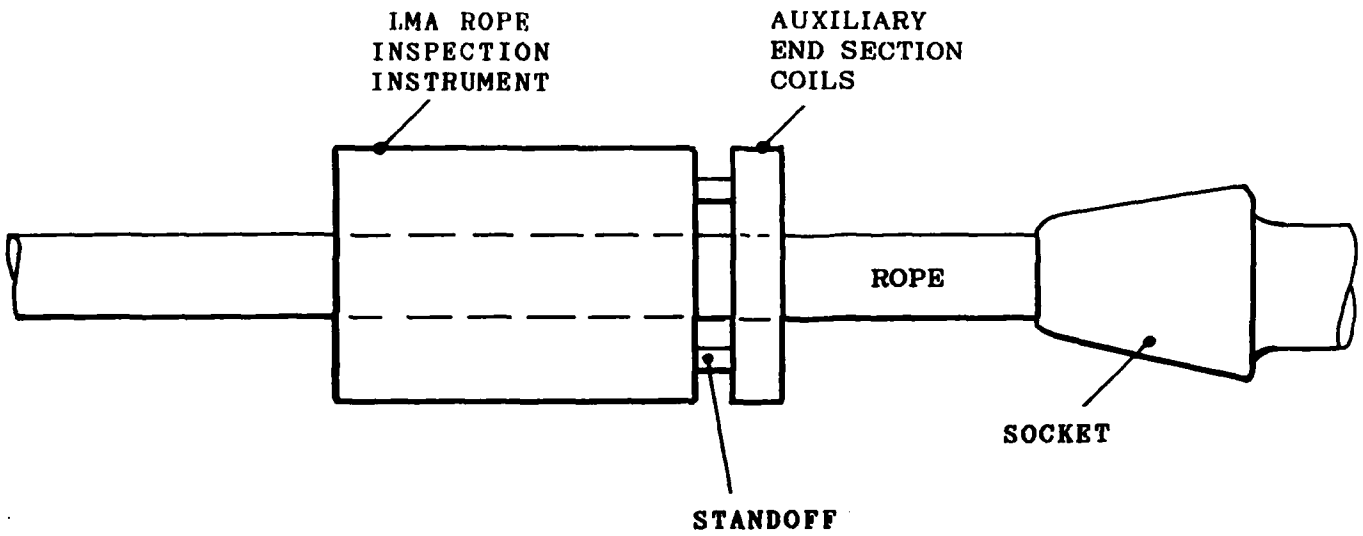

Figure 28: Instrumentation for the Inspection of Wire Rope End Sections

- A regular rope inspection instrument of the above described LMA type, and

- an auxiliary sense coil assembly.

The auxiliary sense head is separate from the regular rope test instrument. It can be mounted on the instrument as required to inspect rope end sections. The sense coil assembly can now be moved up to the rope termination. Since test signal amplitudes are independent of sense head speed, a complete inspection of the rope end section is possible.

This arrangement makes use of the longitudinal flux density pattern in the rope which was shown in Figure 25. According to this Figure, the magnetic flux in the rope is approximately point symmetric in the immediate vicinity of the pole pieces. Therefore positioning the sense coils on either side of the pole pieces should give approximately identical results. Preliminary experiments confirm this observation. These preliminary data are encouraging. Figure 29 shows the experimental data which were obtained by using a provisional sensor-magnetizer arrangement as shown in Figure 28. As compared to the regular sensor configuration, these results show only a slight deformation of the LMA and LF signals.

This coil arrangement will allow a rope inspection up to approximately a distance of five times the rope diameter from the socket without major difficulties. Toward the end section of the rope, close to the socket, the magnetic field becomes drastically distorted, and a major problem

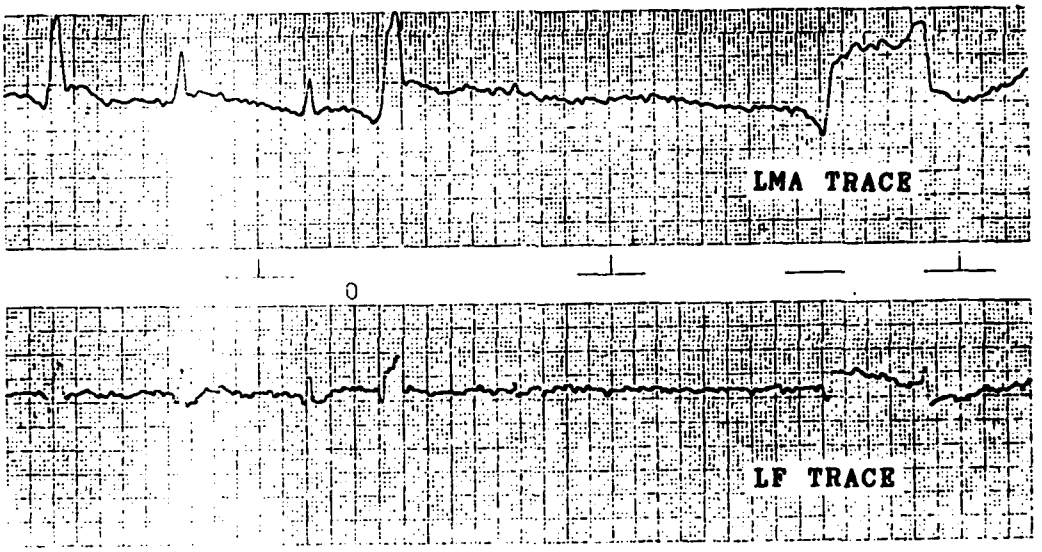

Figure 29: Auxiliary End Section Coils: Preliminary Experimental Results

arises in detecting flaw signals in this distorted field. The present preliminary coil arrangement is not well suited for more extensive investigations of these phenomena. A more permanent end coil arrangement is required and is presently being manufactured. A thorough study was postponed until these new coils will be available.

8. ROPE VELOCITY AND POSITION SENSING

To identify defects quantitatively by using the above described defect identification method, a knowledge of rope velocity is absolutely necessary. In the Phase II Proposal [1], we had proposed a new velocity sensing method without a mechanical tachometer. This method would use the ratio of the time derivative to space derivative of the LMA signal to determine the actual rope speed.

We undertook a major effort to implement this procedure. The proposed method looks simple. However, in spite of the application of fairly sophisticated correlation methods, we were not able to determine the speed with sufficient accuracy. Problems are caused by noise and by the fact that only an approximation of the the spatial derivative of the LMA signal is available.

Since the accurate determination of rope speed is absolutely necessary for the qualitative defect identification, we implemented a conventional speed and position sensor using an incremental optical encoder. This encoder, including signal electronics, is now available.

For the usual applications, this encoder is accurate, convenient, and

reliable. However, in some cases, such as underwater applications, a mechanical encoder may not be practical. For these applications, a rope strand counter was implemented. The strand counter uses a commercial magnetic pickup to sense the strands of the rope as it moves. This approach uses no moving mechanical parts. However, obviously it can be used only for stranded ropes. Since the lay length varies for different ropes, an appropriate scale factor would have to be introduced for velocity and distance measurements for each rope. Nevertheless, this approach is a simple and viable alternative for applications where a rotary mechanical transducer is not feasible.

BIBLIOGRAPHY

[1] H.R.Weischedel, "Electromagnetic Inspection of Wire Ropes Using Sensor Arrays," DESAT/SBIR Phase II Proposal, 1982

[2] H.R.Weischedel, "Electromagnetic Inspection of Wire Ropes Using Sensor Arrays," DESAT/SBIR Phase I Final Report, Contract N00014-82-C-0146, 1982

[3] L.D.Underbakke, "Test and Evaluation of the MT 75 Rope Tester - A Hand-Held NDT Wire-Rope Testing Device," TN NO: N-1661, Naval Civil Engineering Laboratory, Port Hueneme, CA 93043, 1983

[4] R.E.Beissner. G.A.Matzkanin and C.M.Teller, "NDE Application of Magnetic Leakage Field Methods, A State-of-the-Art Survey". Southwest Research Institute, San Antonio, Texas, January 1980

[5] F.Foerster, "Theoretical and Experimental Developments in Magnetic Stray Flux Techniques for Defect Detection," British J. NDT, November 1975, pp. 168-171

[6] H.Babel, "Destructive and Nondestructive Test Methods for the Determination of the Life Expectancy of Wire Ropes, Part II," (in German), Draht, Vol.30, No.4, pp. 354-359, 1979

[7] R.Kurz, "The Magnetic Induction Method for Cable Testing, Experience and Future Prospects," Fourth International Congress of

Transportation by Rope, Vienna, 1965

[8] R.Kurz, "Magnet-Inductive Wire Rope Testing" (in German), Draht-Welt, Vol.51, No.12, pp. 632-638, 1965

[9] M.J.Bergander, "Principles of Magnetic Defectoscopy of Steel Ropes," Wire Journal, pp. 62-67, May 1978

[10] D.N.Poffenroth, "Flaw Detection in Mine Hoist Transportation Systems," First Annual Wire Rope Symposium, Denver, Colorado, March 1980

[11] E.Ulrich and H.Grupe, "The Inspection of Highly Stressed Mine Hoist Ropes" (in German), Glueckauf, Vol.111, No.18, pp. 870-874, 1975

[12] H.Grupe, "Development of a Device for Magnet-Inductive Testing of Hoist-Ropes" (in German), Forschungsberichte des Landes Nordrhein-Westfalen, Westdeutscher Verlag, Koeln-Opladen, 1961

[13] H.Arnold, "Magnet-Inductive Steel Rope Testing, an Aid in Inspecting Installations and Designs with Moving and Stationary Rope Systems" (in German), Der Stahlbau, No.8, pp. 234-240, 1977

[14] H.Grupe, "Magnetinductive Testing Device for Steel Wire Ropes," (in German), Glueckauf, Vol.110, No.23, pp. 993-995, 1974

[15] H.Grupe, "Final Report on the Electromagnetic Tests Conducted with the Financial Support of the European Community" (in German), Luxemburg, 1964

[16] R.Kurz, "Experiences with Magnet-Inductive Rope Testing" (in German), Draht-Welt, Vol.20, No.4, pp. 129-133, 1974

[17] U.B.Meyer, "Electromagnetic Testing of Wire Ropes" (in German), Mitteilungen aus dem Institut fuer Elektrische Maschinen an der ETH, Professor A.Dutoit, Editor, Juris Druck und Verlag, Zuerich, 1973

[18] J.Stachurski and M.Bergander, "Theoretical Approach of Calibration of Defectograph with Integrating Recording", The First International Symposium on Non-Destructive Testing of Steel Ropes, Cracow, Poland, June 1974

[19] W.Hackenberg, "Possibilities for Monitoring Ropes in Mine Hoists", (in German), Glueckauf, Vol.115, No.18, pp. 902-904, 1979

[20] J.R.Wait, "Review of Electromagnetic Methods in Nondestructive Testing of Wire Ropes," Proc. of the IEEE, Vol.67, No.6, pp. 892-903, June 1979

[21] T.Harvey and H.W.Kruger, "The Theory and Practice of Electronic Testing of Winding Ropes," Trans.S.A.Inst.Electr. Engineers, Vol.5, No.6, June 1959

[22] W.Rieger, "A Contribution to the Magnetinductive Cross-Sectional Area Measurement of Wire Ropes" (in German), Doctoral Dissertation, Univesitaet Stuttgart, Germany, 1983.

[23] F.Kitzinger and J.R.Naud, "New Developments in Electromagnetic Testing of Wire Rope," Canadian Mining and Metallurgical Bulletin, June 1979

[24] L.D.Underbakke and H.H.Haynes, "Test and Evaluation of the Magnograph Unit - A Nondestructive Wire Rope Tester,"TN NO: N-1639, Naval Engineering Laboratory, Port Hueneme CA, 1982

[25] P.Aimone, "Nondestructive Testing of Wire Ropes in the Mining Industry," 85th Annual General Meeting of CIM - 1983, Paper No. 66

END

FILMED

2-85

DTIC